THE ASTROPHYSICAL JOURNAL, 326:490–508, 1988 March 1

THE PREDICTED ABUNDANCES OF DEUTERIUM-BEARING GASES IN THE ATMOSPHERES OF JUPITER AND SATURN

BRUCE FEGLEY, JR., AND RONALD G. PRINN
Department of Earth, Atmospheric, and Planetary Sciences, Massachusetts Institute of Technology
Received 1987 April 6; accepted 1987 August 14

ABSTRACT

Results are presented for the first comprehensive set of thermochemical calculations of isotopic exchange reactions for D/H, $^{13}C/^{12}C$, $^{15}N/^{14}N$, and $^{18}O/^{16}O$ in the hot, deep atmospheres of Jupiter and Saturn. Baseline models consistent with the observational constraints on atmospheric thermal profiles, isotopic ratios, and chemical compositions were employed; the sensitivity of the results to variations in elemental and isotopic abundances was studied. A wide range of assumed vertical eddy diffusion coefficients was used in the models; baseline values of 2×10^8 cm^2 s^{-1} were selected. In addition to HD and CH_3D, which have already been observed, the most abundant deuterium-bearing gases in the atmospheres of Jupiter and Saturn are predicted to be HDO, NH_2D, and HDS. All other deuterium-bearing gases have volume mixing ratios $\leq 10^{-9}$, the more abundant of these being PH_2D, DCl, CH_2D_2, DF, and D_2O. Quenching of D/H exchange reactions for CH_3D, HDO, NH_2D, DCl, DF, and DCN was studied quantitatively; the resulting quench temperatures (T_Q) are in the 700–1000 K range for K = 2×10^8 cm^2 s^{-1}. The calculated quench temperatures and deuterium fractionation factors are independent of the assumed elemental enrichments over solar composition and the assumed D/H ratio. Our results for CH_3D fractionation factors on Jupiter differ importantly from those of Beer and Taylor. These gases are isotopic probes of the deep atmospheres of Jupiter and Saturn and sample regions intermediate between those probed by CO, PH_3, N_2, and GeH_4 ($T_Q \sim$ 1000–1600 K) and by ortho-para transitions in H_2 ($T \sim$ 130–160 K). Quenching of the $^{13}C/^{12}C$, $^{15}N/^{14}N$, and $^{18}O/^{16}O$ ratios in several nonequilibrium trace gases (CO, CO_2, N_2, HCN) gives fractionations of several parts per thousand relative to the isotopic ratios in the major reservoirs (e.g., CH_4, NH_3, and H_2O) and can distinguish in principle between photochemical sources in the upper atmospheres and thermochemical sources in the lower atmospheres for these gases. The calculated fractionation factors do not depend on the absolute values of the isotopic ratios involved. These calculations also demonstrate that contrary to popular belief the vertical transport of HCN from Jupiter's deep atmosphere provides an HCN mixing ratio of $\sim 10^{-9}$, consistent with the observed HCN abundance of (1–4) $\times 10^{-9}$ reported by Tokunaga *et al.* Finally, an exhaustive examination of possible processes responsible for the apparent discrepancies between D/H ratios derived from available observations of HD and CH_3D on Jupiter and Saturn implies that D/H ratios from the available HD observations are incorrect.

Subject headings: deuterium — planets: abundances — planets: atmospheres — planets: Jupiter — planets: Saturn

I. INTRODUCTION

The major reservoir of deuterium in the atmospheres of Jupiter and Saturn is HD (e.g., see Macy and Smith 1978; McKellar, Goetz, and Ramsay 1976; Trauger *et al.* 1973; Trauger, Roesler, and Mickelson 1977). Exchange of deuterium in this reservoir with hydrogen combined in CH_4, H_2O, NH_3, H_2S, and other hydrides via equilibria such as

$$CH_4 + HD = CH_3D + H_2 , \quad (1)$$

$$H_2O + HD = HDO + H_2 , \quad (2)$$

$$NH_3 + HD = NH_2D + H_2 , \quad (3)$$

$$H_2S + HD = HDS + H_2 \quad (4)$$

leads to the production of other, less abundant deuterium-bearing gases. Indeed, CH_3D has been observed in the atmospheres of Jupiter and Saturn (Beer and Taylor 1973, 1978*a*; Bjoraker, Larson, and Kunde 1986*a*; Courtin *et al.* 1984; Drossart *et al.* 1982; Fink and Larson 1978; Knacke *et al.* 1982; Kunde *et al.* 1982) at volume mixing ratios of $\sim$(1.8–3.6) $\times 10^{-7}$ on Jupiter and $\sim$(1.2–3.9) $\times 10^{-7}$ on Saturn.

Thermodynamic treatments of isotopic exchange equilibria (Kirshenbaum 1951; Richet, Bottinga, and Javoy 1977; Urey 1947) show that the equilibrium constants for such reactions are different from unity and vary in a predictable fashion as a function of temperature. Beer and Taylor (1973, 1978*a*) used these considerations to demonstrate that the CH_3D observed on Jupiter can be produced via reaction (1) in the deep atmosphere of that planet. By analogy, the same situation is expected to be true on Saturn as well. Furthermore Beer and Taylor (1973) also suggested that reaction (1) may be quenched at different temperatures (and thus at slightly different CH_3D/CH_4 ratios) as a function of the assumed vertical mixing rate in Jupiter's deep atmosphere (quench temperatures of $\sim$700–900 K in their model). In other words, CH_3D is an isotopic probe of the deep atmospheres of Jupiter and Saturn. Such isotopic probes may provide information on vertical mixing rates complementary to that potentially available from the proposed chemical probes (e.g., PH_3, GeH_4, CO, HCN, N_2) of atmospheric dynamics on Jupiter and Saturn (Fegley and Prinn 1985; Prinn and Barshay 1977; Prinn and Olaguer 1981).

However, the interpretation of isotopic ratio observations on Jupiter and Saturn is presently limited by the lack of any detailed thermochemical-dynamical model for isotopic exchange reactions in the deep atmospheres of these planets. Also, more recent and more accurate thermodynamic and kinetic data on reaction (1) and the relevant reaction pathways are available since the work of Beer and Taylor on CH_3D and permit a much improved description of this important isotopic probe.

In this paper we present the first set of comprehensive thermochemical equilibrium and chemical kinetic calculations on the chemistry of deuterium-bearing gases in the deep atmospheres of Jupiter and Saturn. The results of the calculations are useful for several purposes including (*a*) interpreting the abundance of the observed CH_3D in terms of vertical mixing from specific atmospheric levels, (*b*) predicting other potentially observable deuterium-bearing gases, (*c*) predicting the fractionation factors for deuterium exchange between HD and important gaseous hydrides (e.g., CH_4, H_2O, NH_3) as a function of assumed vertical mixing rates, (*d*) predicting isotopic fractionations due to the condensation of cloud-forming materials, and (*e*) using the derived D/H ratios for Jupiter and Saturn to contrast and evaluate models for their origin, evolution, and composition.

We also consider briefly isotopic fractionation effects in the $^{13}C/^{12}C$, $^{15}N/^{14}N$, and $^{18}O/^{16}O$ ratios in nonequilibrium species such as CO, CO_2, HCN, and N_2 (relative to the respective ratios in CH_4, H_2O, NH_3). In principle, such effects can distinguish between photochemical sources in the upper atmospheres and thermochemical sources in the lower atmospheres of Jupiter and Saturn for these species.

Finally, we note that both HD and CH_3D have also been observed on Uranus (DeBergh *et al.* 1986; Macy and Smith 1978; McKeller, Goetz, and Ramsay 1976; Trafton and Ramsay 1980). However, the thermodynamics and kinetics of deuterium exchange reactions on Uranus are not covered in this paper because the nonideality of the cold, dense Uranus atmosphere and the expected large enrichments in H_2O, CH_4, NH_3, etc. (see Fegley and Prinn 1986 and references therein), lead to effects beyond the scope of the present treatment.

II. ATMOSPHERIC MODELS

a) Pressure-Temperature Profiles

Our calculations for these two planetary atmospheres utilize baseline models which are consistent with recent observational constraints on their chemical compositions, D/H ratios, and thermal structures. However, the influence of varying atmospheric chemical compositions, D/H ratios, and vertical mixing rates was also studied.

Both Jupiter and Saturn have internal heat sources resulting in high internal temperatures and deep convective atmospheres (Hubbard and Stevenson 1984 and references therein). Adiabatic temperature gradients were therefore assumed below the respective tropopauses on the two planets. Dry adiabatic lapse rates in the deep atmospheres were calculated stepwise using the methods described by Fegley and Prinn (1985) with the following parameters: (*a*) Jupiter: temperature at 1 bar = 165 K (Lindal *et al.* 1981), H_2 and He volume mixing ratios of 0.90 and 0.10 (Conrath *et al.* 1984; Gautier *et al.* 1981), average gravitational acceleration of 2600 cm s^{-2}; (*b*) Saturn: temperature at 1 bar = 136 K (Prinn *et al.* 1984), H_2 and He volume mixing ratios of 0.932 and 0.068 (Prinn *et al.* 1984), average gravitational acceleration of 1117 cm s^{-2}. The temperature dependence of the heat capacity at constant pressure for H_2 was taken into account in the calculations.

The dry adiabats in the 200–300 K region will be modified slightly by latent heat effects due to condensation of NH_4HS(s), aqueous solution, and water ice clouds (e.g., see Lewis and Prinn 1984; Prinn *et al.* 1984; Romani 1986). These effects were calculated to a sufficient approximation for our purposes using the wet adiabatic lapse rate given by Fegley and Prinn (1986) and vapor pressure data for pure liquid water and water ice (Keenan *et al.* 1969; Mason 1971). Below the H_2O (s, l) cloud base, the water vapor mixing ratios in our baseline models are enhanced over the solar value (Cameron 1982) by factors of 2.3 and 2.5 times for Jupiter and Saturn, respectively. These choices are discussed further in § II*b*.

The vertical scales in Figures 1 and 2 illustrate the resultant pressure-temperature profiles and depth scales for the Jupiter and Saturn baseline models. The results for Saturn are the same as those given previously (Fegley and Prinn 1985), while the results for Jupiter differ slightly from those given by Barshay and Lewis (1978) for a pre-Voyager model atmosphere with solar composition (Cameron 1973). For reference, the calculated pressures at 300 K in our baseline models are 7.4 bars for Jupiter and 13.5 bars for Saturn. These values agree reasonably well with Romani's (1986) results at 300 K of 6.8 bars for Jupiter and 13.5 bars for Saturn.

b) Chemical Compositions

We have adopted the chemical model for Saturn's atmosphere that was given by Fegley and Prinn (1985). The H_2 and He volume mixing ratios are 0.932 and 0.068, respectively, while the mixing ratios of all other elements are set equal to 2.5 times their solar composition values (Cameron 1982). This choice is based on the critical review of Earth-based, Earth-orbital, and Voyager spectroscopic observations presented by Prinn *et al.* (1984). Conrath *et al.* (1984) subsequently derived from Voyager data slightly different volume mixing ratios of 0.963 for H_2 and 0.037 for He. However, use of this revision would not significantly alter our conclusions; the calculated pressure at our maximum temperature of 2000 K would be only 7% larger and the calculated hydrogen fugacity would be only 3% larger at all temperatures.

A similar chemical model has been adopted for the atmosphere of Jupiter. The H_2 and He mixing ratios are 0.90 and 0.10, respectively, the carbon mixing ratio is set equal to the observed CH_4 mixing ratio, which is about 2.3 times the solar value (Gautier and Owen 1983; Gautier *et al.* 1982), and the mixing ratios of all other elements are also set equal to 2.3 times their solar composition values (Cameron 1982). We argue elsewhere (Fegley and Prinn 1987, 1988) that the *apparent* depletion of H_2O in Jupiter's visible atmosphere (Bjoraker, Larson, and Kunde 1986*b*) cannot be due to a bulk global depletion of H_2O on Jupiter but must be due to condensation and/or complex line formation effects.

c) Deuterium to Hydrogen Ratios

We have adopted a D/H ratio of 2.0×10^{-5} for both Jupiter and Saturn in our baseline models. This value is the estimated D/H ratio for the solar nebula (Black 1973; Geiss and Bochsler 1981; Geiss and Reeves 1972) and is therefore an appropriate choice for Jupiter and Saturn, which are believed to have retained the D/H ratio representative of the solar nebula (e.g., see Hubbard and MacFarlane 1980). Furthermore a D/H ratio

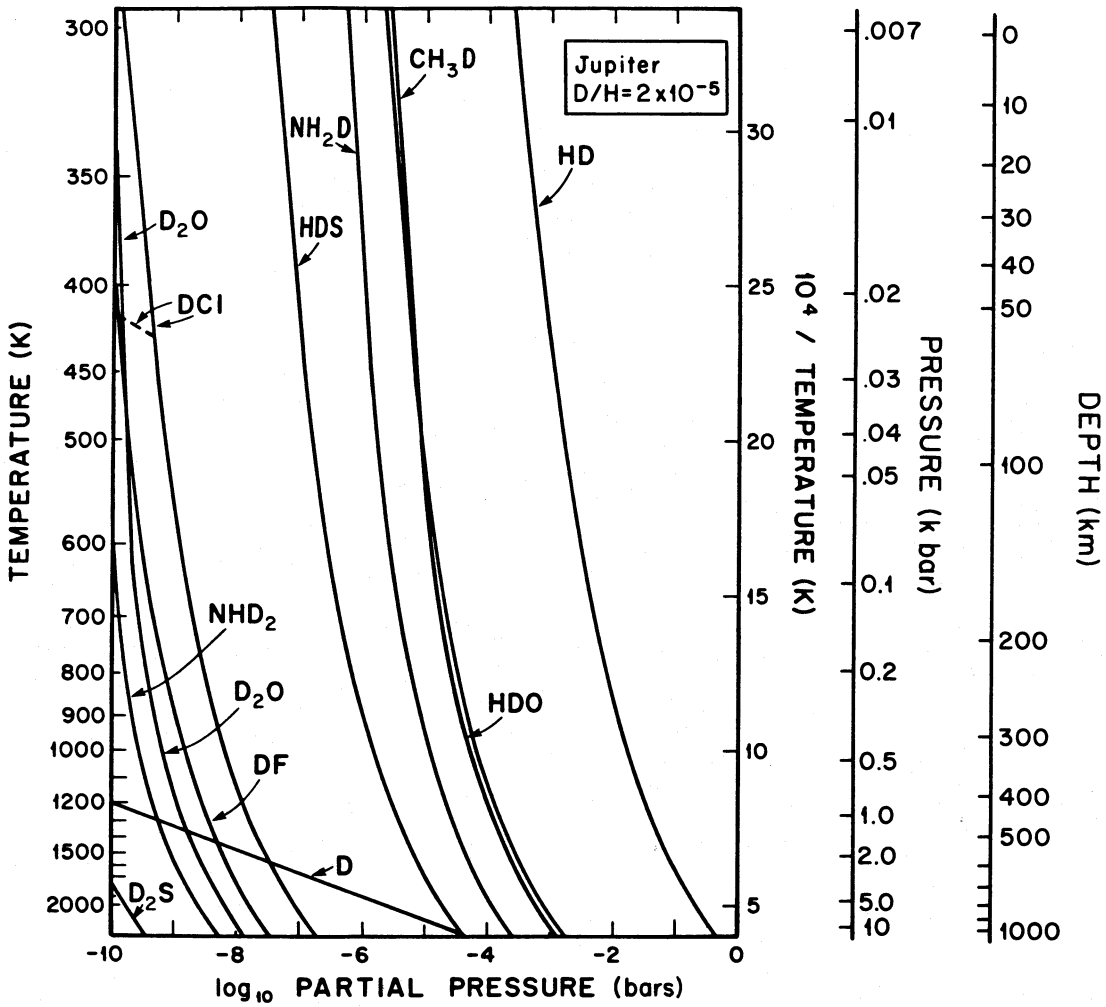

FIG. 1.—Equilibrium abundances of some deuterium-containing gases along the model adiabatic (P, T) profile in Jupiter's atmosphere. The partial pressures are plotted as a function of inverse temperature. Calculations are done for a D/H atom ratio of 2×10^{-5}. The vertical scales indicate temperature, pressure, and depth (below the 300 K level) along the model adiabat. Note that the abundance of HDO is approximately equal to, but slightly less than, the abundance of CH_3D at all levels below the predicted water-bearing cloud base.

of 2×10^{-5} is within the range of D/H ratios of $\sim(1.2$–$10) \times 10^{-5}$ derived from observations of HD and CH_3D on Jupiter and Saturn (Bjoraker, Larson, and Kunde 1986*a*; Courtin *et al.* 1984 and references therein).

d) Calculated Chemical Models

Models of thermochemical equilibrium and (where relevant) nonequilibrium chemistry in the deep atmospheres of Jupiter and Saturn are an essential part of the present work; comprehensive descriptions of the models we have used are given elsewhere (Barshay and Lewis 1978; Fegley and Prinn 1985; Prinn and Barshay 1977; Prinn and Olaguer 1981; Prinn *et al.* 1984). Therefore, only a brief review is given here.

The chemical elements included in our calculations are H, He, O, C, Ne, N, Mg, Si, Fe, S, Ar, Al, Ca, Na, Ni, P, Cl, F, Ge, and Se, which were chosen on the basis of their solar abundance and volatility. Thermodynamic data for these calculations were taken from standard sources (Chase *et al.* 1985; Glushko *et al.* 1965–1981; Glushko *et al.* 1978–1982; Kelley 1937, 1960; Kelley and King 1961; Stull, Westrum, and Sinke 1969; Wagman *et al.* 1968). Approximately 350 (nondeuterated) compounds (see appendices to Barshay and Lewis 1978; Fegley and Lewis 1979) have been considered.

The thermodynamic equilibrium calculations were done by simultaneously considering the constraints of mass balance and chemical equilibrium. Calculations of gas phase and gas-solid, liquid equilibria were done at appropriately spaced temperatures (≤ 100 K intervals) from ~ 200 to 3000 K along the calculated Jupiter and Saturn adiabats. The computations take about 5 minutes (per run) on an IBM XT personal computer or equivalent system. The results for nondeuterated species are discussed elsewhere in connection with vertical mixing on Jupiter and Saturn (Fegley and Prinn 1985) and with constraints on the H_2O and total oxygen abundances on Jupiter (Fegley and Prinn 1988).

III. THERMODYNAMICS OF DEUTERIUM EXCHANGE REACTIONS

a) Method of Calculation

The thermochemical equilibrium abundances of deuterium-bearing gases were calculated as a function of temperature and pressure in the Jupiter and Saturn baseline model atmospheres

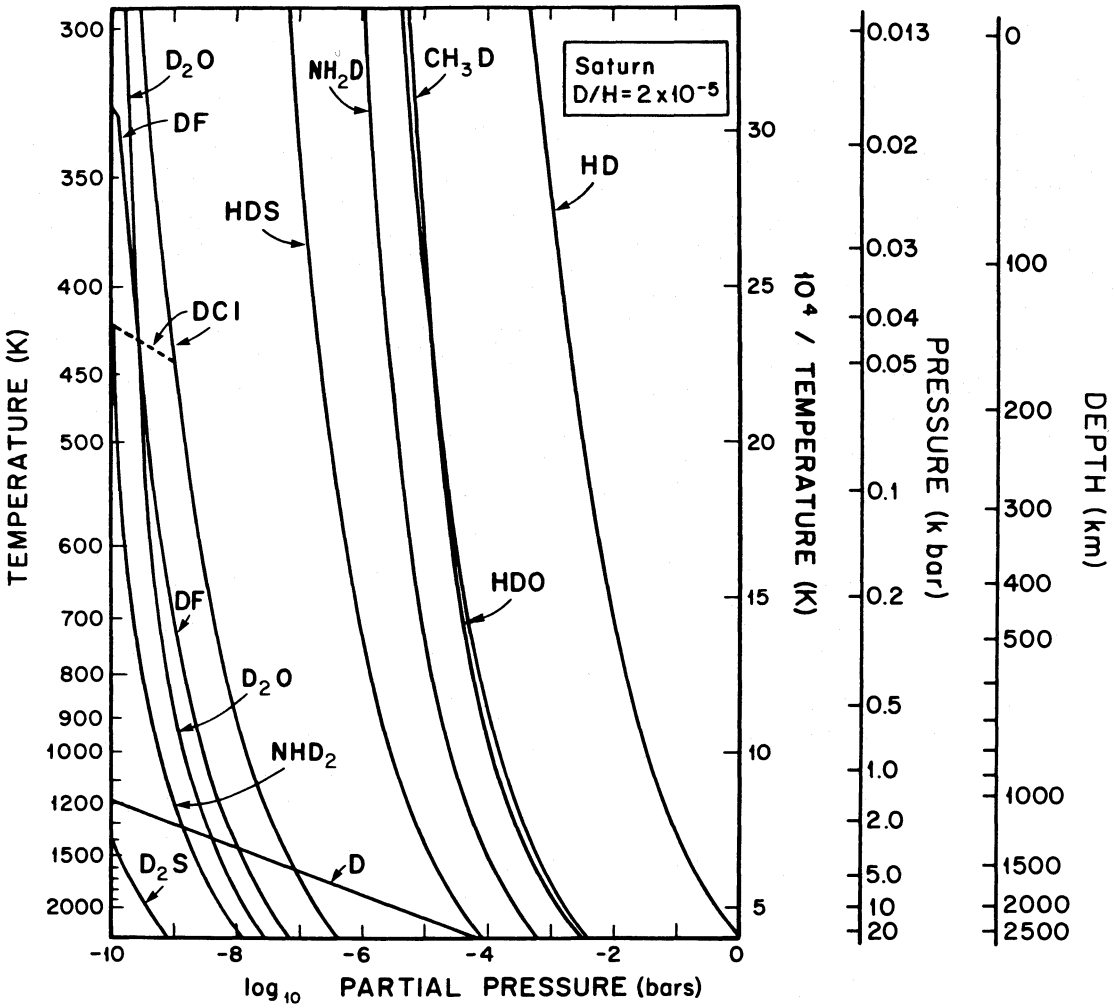

FIG. 2.—As in Fig. 1 but for the model adiabatic (P, T) profile in Saturn's atmosphere

using the standard methods described by Barshay and Lewis (1978). The 32 gases included in the calculations and the thermodynamic data sources used are as follows: CD, CD_2, CD_3, CD_4, CHD_3, CH_2D_2, CH_3D, C_2D_2, C_2D_4, C_2D_6, DCN, D, D_2, DF, DCl, DBr, DI, HD, HDO, D_2O, DO, D_2O_2, DN, ND_2, ND_3, N_2D_2, NH_2D, NHD_2, PH_2D, DS, HDS, D_2S (Burcat 1984; Chase *et al.* 1985; Glushko *et al.* 1965–1981; Glushko *et al.* 1978–1982; Kirshenbaum 1951; Pamidimukkala, Rogers, and Skinner 1982; Richet, Bottinga, and Javoy 1977; Shabur *et al.* 1969; Thyagarajan, Sundaram, and Cleveland 1960; Weston and Bigeleisen 1952). Table 1 summarizes the thermodynamic data sources for all the deuterium-bearing gases that were included in our calculations. The thermodynamic data in these references are in a variety of formats such as reduced partition functions, equilibrium constants, and fractionation factors, which are interrelated as described by Kirshenbaum (1951), Richet, Bottinga, and Javoy (1977), and Urey (1947), among others.

For our purposes it is sufficient to note that the fractionation factor α is defined as

$$\alpha_{gas} = [(D/H)_{gas}]/[(D/H)_{H_2}] , \quad (5)$$

where the terms in parenthesis denote the (D to H) atom ratios in the two phases and the subscript gas stands for CH_4, H_2O,

TABLE 1

THERMODYNAMIC DATA SOURCES FOR SELECTED DEUTERIUM-BEARING GASES

Gas	References
CD, CD_2, CD_3, CD_4	1
CHD_3, CH_2D_2	1
CH_3D, NH_2D, HDS, DCl, DF, DCN	2
C_2D_2, C_2D_4, C_2D_6	3
D, D_2, HD, HDO, D_2O, DO	4
DN, ND_2, ND_3, N_2D_2, DS, D_2S	4
DBr, DI, D_2O_2	5
NHD_2	6
PH_2D	7, 8, 9, 10

REFERENCES.—(1) Burcat 1980, 1984, equilibrium constants; (2) Richet, Bottinga, and Javoy 1977, reduced partition functions and the corresponding fractionation factors calculated from them; (3) Pamidimukkala, Rogers, and Skinner 1982, equilibrium constants; (4) JANAF Tables, Chase *et al.* 1985, equilibrium constants; (5) Glushko *et al.* 1978–82, Vol. 1, equilibrium constants corrected to JANAF reference states; (6) Kirshenbaum 1951, reduced partition functions and the corresponding fractionation factors calculated from them; (7) Glushko *et al.* 1965–81, Vol. 3 for ΔH_f^0 (298) corrected to red phosphorus reference state; (8) Thyagarajan, Sundaram, and Cleveland 1960 for free energy functions; (9) Shabur *et al.* 1969 for free energy functions; (10) Weston and Bigeleisen 1952, fractionation factors.

NH_3, H_2S, etc. The relationships between the equilibrium constants for exchange reactions (1)–(4) and the respective α values yield the following equivalent expressions for the D/H atom ratios on Jupiter and Saturn:

$$(D/H) \sim (X_{CH_3D}/X_{CH_4})/4\alpha_{CH_4} , \quad (6)$$

$$(D/H) \sim (X_{HDO}/X_{H_2O})/2\alpha_{H_2O} , \quad (7)$$

$$(D/H) \sim (X_{NH_2D}/X_{NH_3})/3\alpha_{NH_3} , \quad (8)$$

$$(D/H) \sim (X_{HDS}/X_{H_2S})/2\alpha_{H_2S} , \quad (9)$$

where X_i is the volume mixing ratio for species i and α_i is the D/H fractionation factor for species i as defined by equation (5). Certain approximations are made in deriving equations (6)–(9) (Kirshenbaum 1951), but the errors introduced are insignificant at D/H atom ratios $\leq 10^{-2}$, which is the case on Jupiter and Saturn. Equations (6)–(8) can be used in conjunction with the fractionation factors in Figures 3–5 to derive the

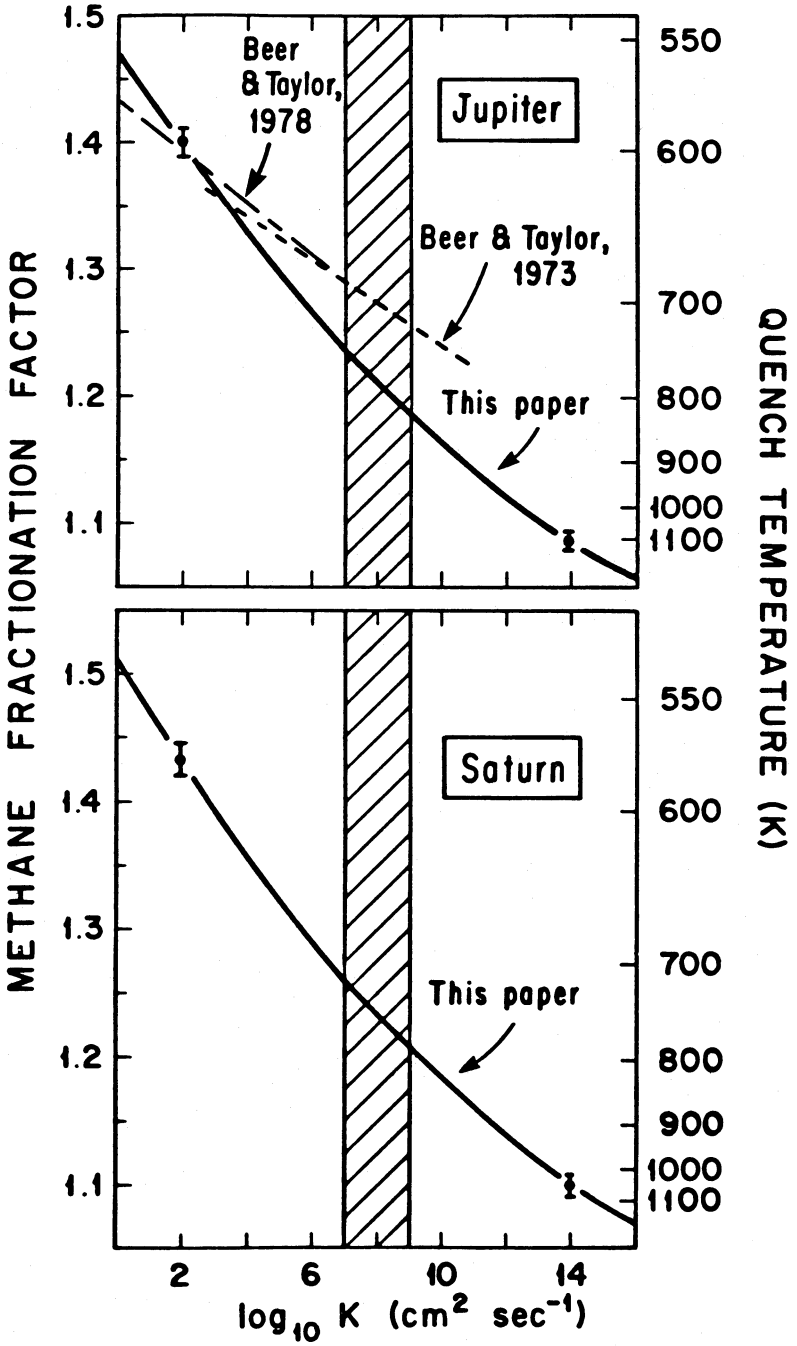

FIG. 3.—Predicted fractionation factors for deuterium exchange between CH_4 + HD in the atmospheres of Jupiter and Saturn as a function of the vertical eddy diffusion coefficient K. The fractionation factor is defined as the D/H atom ratio in methane relative to the D/H atom ratio in hydrogen and is tabulated as a function of temperature by Richet, Bottinga, and Javoy (1977). The calculated quench temperatures for CH_3D formation via homogeneous gas phase deuterium exchange are also shown. The shaded regions at $K = 10^7$–10^9 cm^2 s^{-1} are appropriate for independent estimates of K in the deep atmospheres of Jupiter (Flasar and Gierasch 1977; Stone 1976) and Saturn (Prinn *et al.* 1984). The error bars on the solid curves illustrate the effect of uncertainties of a factor of 2 in the kinetic data on the resulting fractionation factors and quench temperatures. See the text for a discussion of the results of Beer and Taylor (1973, 1978*a*).

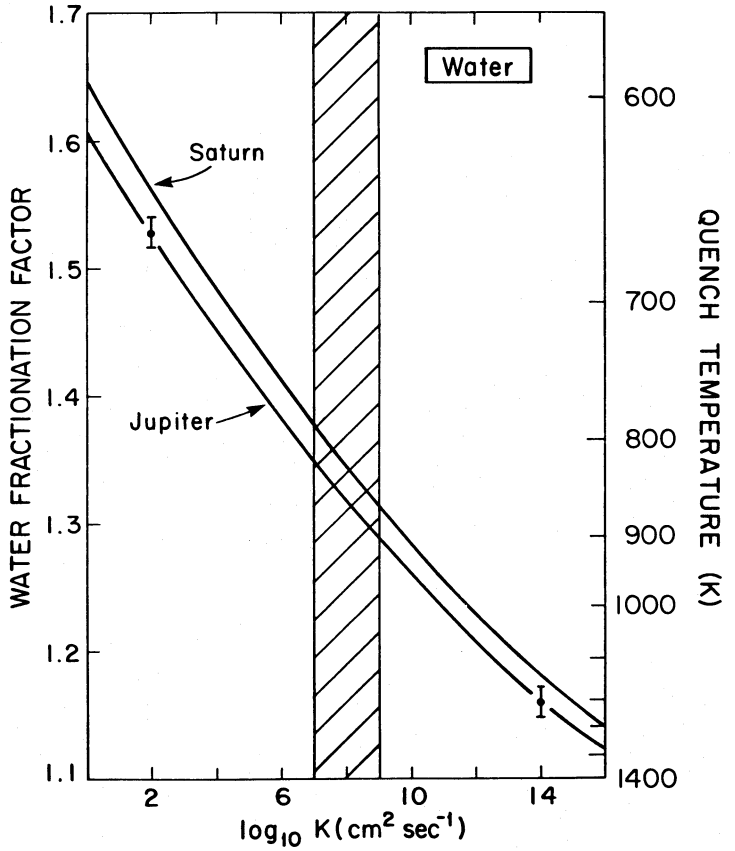

FIG. 4.—As in Fig. 3 but for deuterium exchange between H_2O + HD. The indicated uncertainties apply to both the Jupiter and Saturn curves.

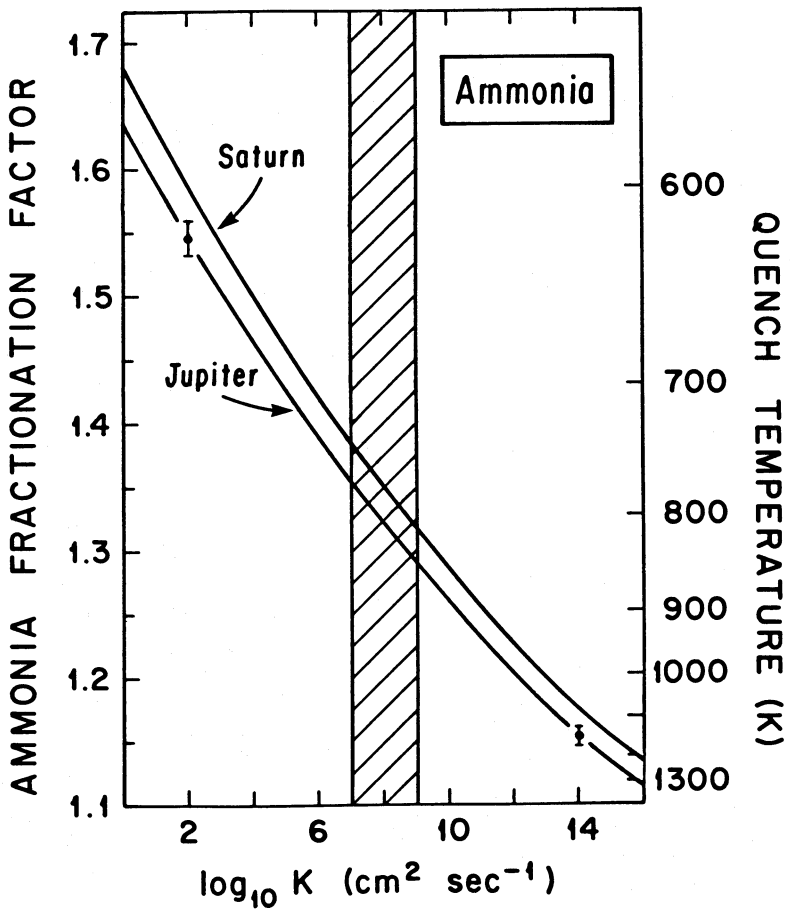

FIG. 5.—As in Fig. 3 but for deuterium exchange between NH_3 + HD. The indicated uncertainties apply to both curves.

D/H ratios on Jupiter and Saturn from observations of CH_3D, HDO, and NH_2D. Equivalent expressions can be derived for the analogous exchange reactions producing DF, DCl, DBr, DI, DCN, and PH_2D, but, as we discuss below, the predicted abundances of these gases are probably below present-day remote sensing capabilities.

b) Results

The calculated equilibrium abundances of the major deuterium-bearing gases on Jupiter and Saturn are illustrated in Figures 1 and 2, where the partial pressures of the various gases are plotted as a function of inverse temperature along the calculated adiabatic (P, T) profiles.

The only thermochemically produced deuterium-bearing gases with mixing ratios greater than 10^{-9} throughout the entire temperature range considered are predicted to be HD, CH_3D, HDO, NH_2D, and HDS. Although only HD and CH_3D have been observed so far, we emphasize the similar abundances predicted for HDO and CH_3D below the water-bearing cloud base. However, given the observed low H_2O mixing ratios on Jupiter (Bjoraker, Larson, and Kunde 1986*b*) and the stringent upper limits (Larson *et al.* 1984; Fink and Larson 1979) for H_2S in the observable regions of the atmospheres of Jupiter ($X_{H_2S} < 3.3 \times 10^{-8}$) and Saturn ($X_{H_2S} < 1.4 \times 10^{-6}$), perhaps NH_2D is the best candidate for detection by remote sensing, although it may not be observable at millimeter wavelengths (Lellouch and Destombes 1985).

Other than a few highly reactive atoms and radicals (e.g., D atoms), the only deuterium-bearing gases predicted to have mixing ratios between 10^{-12} and 10^{-9} in the deep atmospheres of Jupiter and Saturn are PH_2D, DCl, CH_2D_2, DF, and D_2O. The predicted abundances of other deuterium-bearing gases (e.g., GeH_3D) are even lower. For the sake of completeness, the predicted mixing ratios at 1000 K for PH_2D and CH_2D_2 (neither of which are graphed) are $\sim 5.9 \times 10^{-11}$ and $\sim 4.0 \times 10^{-12}$ on Jupiter and $\sim 5.3 \times 10^{-11}$ and $\sim 4.4 \times 10^{-12}$ on Saturn. The apparent quenching of the PH_3 to P_4O_6 conversion will yield increasing PH_2D mixing ratios with decreasing temperature; representative values assuming $D/H = 2.0 \times 10^{-5}$ are $\sim 1.2 \times 10^{-10}$ and $\sim 1.3 \times 10^{-10}$ at 300 K on Jupiter and Saturn. However, the observation of any of these trace deuterium-bearing gases having mixing ratios below 10^{-9} is likely to be extremely difficult at the present time.

As illustrated in Figures 1 and 2, the calculated CH_3D/HDO ratios are greater than unity despite a CH_4/H_2O ratio of 0.73 in both baseline models. This reversal is due to the presence of twice as many exchangeable H atoms in CH_4 than in H_2O, as can be seen by equating and rearranging equations (6) and (7):

$$(X_{CH_3D}/X_{HDO}) = 2(X_{CH_4}/X_{H_2O})(\alpha_{CH_4}/\alpha_{H_2O}) . \quad (10)$$

However, the calculated CH_3D/HDO ratio is ~ 1.3 times the assumed CH_4/H_2O ratio instead of 2 times this ratio because $\alpha_{CH_4} < \alpha_{H_2O}$, as shown by the data in Richet, Bottinga, and Javoy (1977). The larger CH_3D/HDO ratio is still found if a CH_4/H_2O ratio of ~ 0.6 (which neglects the oxygen incorporated into rocky material) is assumed.

Similarly, the calculated NH_2D/HDO ratio is greater than the assumed NH_3/H_2O ratio by a factor of ~ 1.5 as expected from a combination of equations (7) and (8) giving

$$(X_{NH_2D}/X_{HDO}) = 1.5(X_{NH_3}/X_{H_2O})(\alpha_{NH_3}/\alpha_{H_2O}) , \quad (11)$$

because $\alpha_{NH_3} \sim \alpha_{H_2O}$ over the temperature range considered (Richet, Bottinga, and Javoy 1977). Finally, the calculated HDS/HDO ratio is less than the assumed H_2S/H_2O ratio by a factor proportional to the ratio of the two α values because both molecules have two exchangeable H atoms.

Another important feature illustrated by our equilibrium calculations is that stable deuterium-bearing gases such as CH_3D, HDO, NH_2D, and HDS are slightly more abundant at lower temperatures than at higher temperatures. For example, the calculated ratios of CH_3D/CH_4, HDO/H_2O, NH_2D/NH_3, and HDS/H_2S at 300 K relative to the same ratios at 2000 K are 2.9, 3.0, 3.5, and 1.6, respectively, on both Jupiter and Saturn. Similar increases are observed in the ratios of PH_2D/PH_3, NHD_2/NH_3, CH_2D_2/CH_4, DCl/HCl, DF/HF, etc. However, in the latter two cases the increases are terminated by the condensation of NH_4Cl (~ 429 K on Jupiter and ~ 440 K on Saturn) and NH_4F (~ 320 K on Jupiter and ~ 328 K on Saturn).

Inspection of equations (6)–(9) shows that the temperature dependences of the CH_3D/CH_4, HDO/H_2O, NH_2D/NH_3, and HDS/H_2S ratios are given by equations exemplified by

$$[(X_{NH_2D}/X_{NH_3})_{T_1}]/[(X_{NH_2D}/X_{NH_3})_{T_2}] = \alpha_{T_1}/\alpha_{T_2} , \quad (12)$$

where in this case α is the fractionation factor for NH_3. Thus, the increased abundances of the deuterated gases at lower temperatures are simply a consequence of the more favorable deuterium fractionation factors at lower temperatures (e.g., see Richet, Bottinga, and Javoy 1977) and are independent of the assumed D/H ratio in the planetary atmosphere.

In principle, the temperature- (and thus altitude-) dependent ratios of CH_3D/CH_4, HDO/H_2O, and NH_2D/NH_3, etc. make these deuterium-bearing hydrides potential isotopic probes of the vertical mixing rates in the deep atmospheres of Jupiter and Saturn. In order to explore the utility of this approach, we will now examine in detail the thermochemical kinetics of the elementary reactions involved in the formation of these deuterium-bearing gases.

IV. THERMOCHEMICAL KINETICS OF DEUTERIUM EXCHANGE REACTIONS

a) Estimation of Chemical Time Constants

The effects of vertical mixing on the ratios of CH_3D/CH_4, HDO/H_2O, NH_2D/NH_3, and so on can be calculated quantitatively using a simple chemical-dynamical model developed to describe the effects of vertical mixing on the abundances of nonequilibrium trace gases such as CO, PH_3, GeH_4, HCN, and N_2 (e.g., see Prinn and Barshay 1977; Prinn and Olaguer 1981; Fegley and Prinn 1985). The basic approach used is similar in both cases: the time constant t_{chem} for the dominant reaction producing or destroying a gas or increasing or decreasing the ratio of two gases is compared to the time constant t_{conv} ($\sim H^2/K$, where H is the atmospheric pressure scale height and K is the vertical eddy diffusion coefficient) for convectively mixing the gas to a cooler region higher up in the atmosphere where these reactions will be kinetically inhibited. Thus, in the deeper regions of the atmosphere where $t_{chem} < t_{conv}$, thermochemical equilibrium is maintained, whereas in the upper regions of the atmosphere where $t_{chem} > t_{conv}$, thermochemical equilibrium cannot be reached. Once $t_{chem} \sim t_{conv}$, vertical mixing over a very small altitude increment relative to H results in gas concentrations and ratios being quenched (or frozen in) at the thermochemical equilibrium values prevailing at this level provided the e-folding altitude for t_{chem} is much less

than H. We describe here the approach used to estimate appropriate chemical time constants for CH_3D, HDO, and NH_2D. The same techniques have also been used to estimate t_{chem} values for the gases DCl, DF, and DCN, which receive less emphasis here because of their lower abundances.

Equation (12) illustrates that temperature dependent changes in the CH_3D/CH_4, HDO/H_2O, and NH_2D/NH_3 ratios are independent of the assumed D/H ratio in the planetary atmospheres. Thus, the quenching of the deuterium exchange equilibria (1)–(3) that are responsible for establishing these isotopic ratios is also independent of the assumed D/H ratio. This can be illustrated best with an example for one ratio such as NH_2D/NH_3. In this case the appropriate chemical time constant for altering the NH_2D/NH_3 ratio is given by

$$t_{chem}\left(\frac{NH_2D}{NH_3}\right) = \left(\frac{[NH_2D]}{[NH_3]}\right) \Big/ \left[\frac{d}{dt}\left(\frac{[NH_2D]}{[NH_3]}\right)\right], \quad (13)$$

where $[i]$ is the number density (cm^{-3}) of species i. Equating the destruction rate of NH_3 by deuterium exchange to the production rate of NH_2D, and utilizing $[NH_3] \gg [NH_2D]$ we obtain

$$t_{chem}\left(\frac{NH_2D}{NH_3}\right) = [NH_2D] \Big/ \left(\frac{d}{dt}[NH_2D]\right). \quad (14)$$

The analogous expressions for the chemical time constants for the CH_3D/CH_4 and HDO/H_2O ratios are

$$t_{chem}\left(\frac{CH_3D}{CH_4}\right) = [CH_3D] \Big/ \left(\frac{d}{dt}[CH_3D]\right), \quad (15)$$

$$t_{chem}\left(\frac{HDO}{H_2O}\right) = [HDO] \Big/ \left(\frac{d}{dt}[HDO]\right). \quad (16)$$

The terms $d[i]/dt$ in equations (14)–(16) refer to the net rates of those reactions which tend to restore equilibrium above the quench level. To restore equilibrium, reactions (1)–(3) must proceed specifically to the right; that is, in the direction producing the deuterium-bearing gases DX (where $X = CH_3$, OH, NH_2). Above the quench level, the equilibrating reaction producing DX from HX is exothermic, while the disequilibrating reaction destroying DX to produce HX is endothermic (specifically by ≥ 4 kJ $mole^{-1}$). Also $[HX]$ exceeds its equilibrium value, while $[DX]$ is less than its equilibrium value. As a first-order approximation we therefore ignore the (disequilibrating) reconversion of DX to HX in computing the net rate of DX production above the quench level. To evaluate equations (14)–(16) we therefore need to examine the different elementary reactions responsible for forming C–D, O–D, and N–D bonds in a rising parcel of gas. The approach involved is illustrated here for carbon.

Several elementary reactions may lead to the formation of a C–D bond in a rising gas parcel. Because HD is the major deuterium reservoir, the fastest reaction for doing this may be

$$CH_3 + HD \rightarrow CH_3D + H, \quad (17)$$

where the CH_3 radicals are produced via the equilibria

$$CH_4 = CH_3 + H, \quad (18)$$

$$H + CH_4 = CH_3 + H_2. \quad (19)$$

In this case, the chemical time constant for CH_3D/CH_4 is given by

$$t_{chem}(CH_3D/CH_4) = [CH_3D]/([CH_3][HD]k_{17}) = 2\alpha_{CH_4}/(K_{19}K_{21}^{1/2}k_{17}[H_2]^{1/2}), \quad (20)$$

where α_{CH_4} is defined by equation (5), k_{17} is the rate constant ($cm^3\ s^{-1}$) for reaction (17), K_{19} is the equilibrium constant for reaction (19), and K_{21} is the equilibrium constant for the reaction

$$H_2 = H + H. \quad (21)$$

Both equilibrium constants are defined in terms of molecular number densities. Note that the reverse of reaction (17) is endothermic by ≥ 8 kJ $mole^{-1}$, consistent with our neglect of disequilibrating reactions in computing t_{chem}.

However, if reactions with less abundant deuterium-bearing species yield production rates for CH_3D comparable to that of equation (17) then they may compete effectively with it as a source of CH_3D. In particular, other possible reactions for which kinetic data are available include reactions of CH_3 with HDO, NH_2D, HDS, DCl, and D. The CH_3D production rates for these latter reactions can be calculated to a good first approximation by using molecular number densities from the equilibrium calculations and kinetic data available in the literature (e.g., Tsang and Hampson 1986; Kerr and Parsonage 1976; Baulch *et al.* 1981). Where appropriate, the rate constants are reduced by the statistical factor for D atom abstraction (e.g., by a factor of $\frac{1}{3}$ for reaction with NH_2D) and the kinetic isotope effect is neglected. (However, the kinetic isotope effect has been taken into account for the rate determining reactions in Table 2). The rates so derived for these reactions are substantially smaller than the rate of reaction (17) calculated from the kinetic data in Table 2, and are thus unimportant for determining t_{chem} for CH_3D. In particular, we note that the additional pathway for forming CH_3D via methylene (e.g., $^3CH_2 + HD \rightarrow CH_2D + H$, $CH_2D + H_2 \rightarrow CH_3D + H$) proceeds more slowly than reaction (17) by a factor $\sim[CH_2]/[CH_3](\sim 5 \times 10^{-14}$ at the CH_3D quench temperature $T_Q \sim 790$ K). Furthermore, the rate constants of other possible C–D bond forming reactions, such as reaction of CH_3 with PH_2D for which we could not find any kinetic data, would have to be unreasonably large in comparison with rate constants for analogous reactions for which we have data (e.g., $CH_3 + NH_2D$) in order to be competitive with reaction (17). In other words, the dominance of HD over all other deuterium-bearing gases (e.g., $[HD]/[CH_3D] \sim 100$–200) virtually ensures that reactions with HD will be the fastest reactions for forming C–D, O–D, and N–D bonds in a rising gas parcel.

The importance of reactions with HD was also verified quantitatively for HDO, NH_2D, DCl, DF, and DCN using the same approach as described above for CH_3D. The relevant reactions for all six gases can therefore be written symbolically as

$$X + HD \rightarrow XD + H, \quad (22)$$

where X = OH, NH_2, Cl, F, and CN. The different radicals and atoms involved in reaction (22) may be generated by equilibria such as

$$XH = X + H, \quad (23)$$

$$XH + H = X + H_2, \quad (24)$$

in the rising gas parcels. We verified that these reactions proceed at rates sufficient to insure that thermochemical equilibrium is established on time scales shorter than any feasible time scales for vertical transport.

The chemical time constant expression corresponding to reaction (22) is

$$t_{chem}(XD/XH) = [XD]/([X][HD]k_{22}) = n\alpha_{HX}/(K_{24}K_{21}^{1/2}k_{22}[H_2]^{1/2}), \quad (25)$$

TABLE 2

REACTIONS AND RATE CONSTANTS USED TO ESTIMATE CHEMICAL TIME CONSTANTS FOR SELECTED DEUTERIDE/HYDRIDE RATIOS

Number	Reaction	Rate Constant[a]	$k_{(D/H)}$	Reference(s)[b]
1[c]	$CH_3 + HD \rightarrow CH_3D + H$	$3.0 \times 10^{-22} T^3 \exp(-4050/T)$	$0.27 \exp(-150/T)$	Warnatz 1984
	$CH_3 + H_2 \rightarrow CH_4 + H$	$1.11 \times 10^{-21} T^3 \exp(-3900/T)$		Kerr and Parsonage 1976
2[d]	$OH + HD \rightarrow HDO + H$	$3.7 \times 10^{-18} T^2 \exp(-1740/T)$	$0.345 \exp(-250/T)$	Tsang and Hampson 1986
	$OH + H_2 \rightarrow H_2O + H$	$1.06 \times 10^{-17} T^2 \exp(-1490/T)$		Smith and Zellner 1974
3[e,f]	$NH_2 + HD \rightarrow NH_2D + H$	$1.3 \times 10^{-11} \exp(-6340/T)$	$0.415 \exp(-500/T)$	Michael, Sutherland, and Klemm 1986
	$NH_2 + H_2 \rightarrow NH_3 + H$	$3.07 \times 10^{-11} \exp(-5836/T)$		Kerr and Parsonage 1976
4[g]	$Cl + HD \rightarrow DCl + H$	$1.7 \times 10^{-11} \exp(-2680/T)$	$0.46 \exp(-380/T)$	Baulch *et al.* 1984
	$Cl + H_2 \rightarrow HCl + H$	$3.7 \times 10^{-11} \exp(-2300/T)$		Yaakov, Persky, and Klein 1973
				Persky and Klein 1966
5[h]	$F + HD \rightarrow DF + H$	$7.4 \times 10^{-11} \exp(-730/T)$	$0.48 \exp(-190/T)$	Baulch *et al.* 1981
	$F + H_2 \rightarrow HF + H$	$1.54 \times 10^{-10} \exp(-540/T)$		Persky 1973
6[i]	$CN + HD \rightarrow DCN + H$	$3.8 \times 10^{-11} \exp(-2950/T)$	$0.345 \exp(-250/T)$	Baulch *et al.* 1981
	$CH + H_2 \rightarrow HCN + H$	$1.1 \times 10^{-10} \exp(-2700/T)$		Smith and Zellner 1974

[a] Units for bimolecular rate constants are $cm^3\ s^{-1}$.
[b] The first reference listed gives the corresponding rate constant of the reaction with H_2. Further references give information on the kinetic isotope effect.
[c] $k_{(D/H)}$ for the ratio of the $(CH_3 + HD)/(CH_3 + H_2)$ rates.
[d] $k_{(D/H)}$ is 0.5 times the ratio of the $(OH + D_2)/(OH + H_2)$ rates.
[e] The rate of $NH_2 + H_2$ was calculated from the rate constant for the reverse reaction and the equilibrium constant. The new determinations of the $NH_3 + H$ rate by Michael, Sutherland, and Klemm 1986 and Marshall and Fontijn 1986 agree well with each other.
[f] $k_{(D/H)}$ is 0.5 times the ratio of the $(CH_3 + D_2)/(CH_3 + H_2)$ rates. No data are available for kinetic isotope effects in the $NH_2 + H_2$ reaction.
[g] $k_{(D/H)}$ is the ratio of the $(Cl + HD)/(Cl + H_2)$ rates. The branching ratio of the Cl + HD reaction is also considered.
[h] $k_{(D/H)}$ is 0.5 times the ratio of the $(F + D_2)/(F + H_2)$ rates.
[i] $k_{(D/H)}$ is 0.5 times the ratio of the $(OH + D_2)/(OH + H_2)$ rates. No data are available for kinetic isotope effects in the $CN + H_2$ reaction.

where $n = \frac{1}{2}$ for XD = DCl, DF, and DCN, $n = 1$ for XD = HDO, and $n = 3/2$ for $XD = NH_2D$. The rate constants k_{17} (for CH_3D) and k_{22} (for the X + HD reactions) are given in Table 2. These rate constants take both the required statistical factors and the kinetic isotope effect (e.g., see Melander 1960; Klein 1975) into account as described in the table. However, we note that at temperatures of ~700–1000 K appropriate for quenching reactions (17) and (22) in the deep atmospheres of Jupiter and Saturn (see Table 3 and Figures 3–5), the kinetic isotope effect is a correction on the order of a factor of 2 (i.e., $k_{H_2} \sim 2k_{D_2}$). As the error bars in Figures 3–5 indicate, uncertainties of a factor of 2 do not affect our conclusions in any significant fashion. Finally, we note that reaction (22) is endothermic for the minor gases HDS, PH_2D, DBr, and DI and that reliable kinetic data are unavailable to assess the importance of other possible XD (X = HS, PH_2, Br, I) production reactions. Thus no quenching calculations were done for these four gases.

b) *Vertical Transport of Deuterium-bearing Gases*

Equations (20) and (25) for the chemical time constants, the corresponding rate constants from Table 2, and the relevant molecular number densities from our equilibrium calculations were used to calculate quench temperatures for reactions (17) and (22) by computing the atmospheric level where $t_{chem} \sim t_{conv} \sim H^2/K$ (Prinn and Barshay 1977). The vertical eddy diffusion coefficient K was varied over a wide range to predict abundances of deuterium-bearing gases for different strengths of vertical transport. Our baseline models for Jupiter and Saturn assume $K = 2 \times 10^8\ cm^2\ s^{-1}$, which is consistent with K values of 10^7–$10^9\ cm^2\ s^{-1}$ estimated for the deep atmospheres of these two planets from a knowledge of their internal

TABLE 3

PREDICTED FRACTIONATION FACTORS FOR (D/H) EXCHANGE ON JUPITER AND SATURN[a]

	Jupiter[b]			Saturn[b]		
Gas	Quench Temperature (K)	Fractionation Factor[c] (α)	Predicted Mixing Ratio[d]	Quench Temperature (K)	Fractionation Factor[c] (α)	Predicted Mixing Ratio[d]
CH_3D	790	1.205	1.6×10^{-7}	755	1.229	1.8×10^{-7}
HDO	871	1.310	1.2×10^{-7}	834	1.337	1.3×10^{-7}
NH_2D	818	1.311	2.7×10^{-8}	782	1.341	3.1×10^{-8}
DCl	697	1.062	1.6×10^{-11}	666	1.071	1.7×10^{-11}
DF	982	1.281	2.9×10^{-12}	939	1.305	3.3×10^{-12}
DCN[e]	876	1.166	3.3×10^{-14}	838	1.182	4.0×10^{-15}

[a] For homogeneous gas phase reactions only (see text).
[b] Predictions assume 2.3 times solar composition for Jupiter, 2.5 times for Saturn, and $K_{eddy} = 2 \times 10^8\ cm^2\ s^{-1}$ for both planets.
[c] $\alpha = [(D/H)_{gas}]/[(D/H)_{hydrogen}]$ atom ratio.
[d] Predictions assume $(D/H) = 2 \times 10^{-5}$ for both Jupiter and Saturn. The abundances of the monodeuterides scale linearly with the D/H atom ratio as indicated by equations (6)–(9).
[e] The predicted mixing ratios on Jupiter and Saturn take quenching of HCN into account.

heat fluxes via free convection theory (e.g., see Flasar and Gierasch 1977; Prinn and Owen 1976; Prinn *et al.* 1984; Stone 1976). Note that the K values of 10^7–10^9 cm^2 s^{-1} refer to regions $\sim$1000–2000 km below the visible clouds on Jupiter and Saturn. Values of the vertical eddy diffusion coefficient for the cold, thermochemically inactive visible parts of these two planetary atmospheres are different and are not relevant to our calculations.

The results of our calculations, which are displayed in Table 3 and Figures 3–5, illustrate several important points. First, the predicted quench temperatures (T_Q) for the six deuterium-bearing gases studied (CH_3D, HDO, NH_2D, DCl, DF, DCN) are in the 700–1000 K range. In particular, the predicted quench temperatures for the three most abundant gases (CH_3D, HDO, NH_2D) range from $\sim$800–900 K. Interestingly, this temperature range is between predicted quench temperatures of $\sim$800–1600 K for homogeneous gas phase reactions of CO, CO_2, PH_3, GeH_4, HCN, and N_2 on Jupiter and Saturn (this work and Fegley and Prinn 1985), and predicted quench temperatures of $\sim$130–160 K for the ortho-para transition in H_2 on Jupiter and Saturn (see Congrath and Gierasch 1984 and Massie and Hunten 1982 for opposing points of view). Thus, CH_3D, HDO, and NH_2D (as well as the less abundant deuterides) are potential (isotopic) probes of regions in the deep atmospheres of Jupiter and Saturn that are intermediate between the deeper regions sampled by the chemical probes and the higher regions sampled by ortho-para transitions in H_2.

Note that equations (20) and (25) for the chemical time constants of the various deuteride/hydride ratios show that the t_{chem} and (thus the T_Q) values are dependent only on the fractionation factors α unless either the assumed element enrichments are large enough to significantly alter the H_2 mixing ratio (and the total pressure) or the D/H ratio $\geq 10^{-2}$. Since on Jupiter and Saturn spectroscopic observations indicate (D/H) $\sim 10^{-5}$–10^{-4} and element enrichments only of $\sim$2–5 times solar (Bjoraker, Larson, and Kunde 1986*a*; Courtin *et al.* 1984 and references therein), then the quench temperatures and fractionation factors given in Table 3 and Figures 3–5 are therefore suitable for use with *all* currently accepted chemical models of Jupiter and Saturn.

Our results also show that the predicted T_Q values on Saturn are always slightly lower than those on Jupiter for the same value of the vertical eddy diffusion coefficient. Thus, all fractionation factors on Saturn are slightly larger than their respective values on Jupiter at the same value of the eddy diffusion coefficient. However, the difference ($\sim$2% for CH_3D at $K = 2 \times 10^8$ cm^2 s^{-1}) is smaller than the present uncertainties in the observed CH_3D abundances on both Jupiter and Saturn.

The error bars in Figures 3–5 illustrate the effect of uncertainties of a factor of 2 in the kinetic data on the calculated fractionation factors and quench temperatures. Such uncertainties are typical of those listed for high-temperature kinetic data (e.g., see Warnatz 1984; Tsang and Hampson 1986; Baulch *et al.* 1976, 1981). The resulting effects are larger at lower quench temperatures (i.e., slower assumed vertical mixing rates) than they are at higher quench temperatures (i.e., faster assumed vertical mixing rates). At the baseline K value of 2×10^8 cm^2 s^{-1}, uncertainties of a factor of 2 in the kinetic data typically introduce uncertainties of ± 10 K in the T_Q values and ± 0.010 in the α values. Such small uncertainties are negligible for our purposes and show that our conclusions would not have been significantly altered even if we had neglected totally any corrections for the kinetic isotope effect.

Finally, our results for CH_3D on Jupiter are compared with those of Beer and Taylor (1973, 1978*a*) in Figure 3. Their 1973 results for CH_3D quench temperatures as a function of convective velocity w were plotted versus the eddy diffusion coefficient K ($=wH$) using pressure scale heights calculated from our baseline model. Their 1978 results were plotted assuming that the quoted uncertainty in the α value of 1.37 ± 0.07 corresponded to a range of assumed vertical mixing rates. As Figure 3 illustrates, their replotted α values are larger than our results at all values of the vertical eddy diffusion coefficient $K > 10^{3.5}$ cm^2 s^{-1}. *The reason for the discrepancy is unknown.* However, we note that Beer and Taylor (1973, 1978*a*) used α values for CH_4 from Bottinga (1969), which were later revised by Richet, Bottinga, and Javoy (1977) who discuss the reasons for the revision. Furthermore, their 1973 atmospheric model and chemical kinetic results (e.g., for CH_3D t_{chem} values) are substantially different from those in this work. Naturally we recommend use of our CH_3D fractionation factors given in Table 3 and Figure 3 for interpreting all CH_3D observations on Jupiter and Saturn.

c) *Effects of Heterogeneous Catalysis*

The observational evidence for clouds and aerosols in the atmospheres of Jupiter and Saturn (e.g., see the reviews by Tomasko *et al.* 1984; West, Strobel, and Tomasko 1986) and the possible presence of Fe particles in the deep atmospheres of these two planets (Prinn and Olaguer 1981; Fegley and Prinn 1985) make heterogeneous surface-catalyzed reactions a possibility that must be considered in discussions of atmospheric chemistry. Such reactions are potentially faster than the homogeneous gas phase deuterium exchange pathways and could thus lead to quenching deuterium exchange at lower temperatures and larger fractionation factors (i.e., more deuterium in the various hydride gases).

We consider first the possible Fe catalysis of deuterium exchange reactions between HD and CH_4, H_2O, NH_3, etc., in the deep hot atmosphere. An upper limit to the efficiency of this process is given by the collision lifetime for formation of CH_3D, HDO, NH_2D, etc. Our model utilizes Fe particle number densities and sizes calculated as a function of altitude and vertical mixing rate using the methods described by Prinn and Olaguer (1981). The two model assumptions are (1) that the surfaces of the Fe particles are always covered with hydrogen having a D/H ratio equal to that in the gas phase (2×10^{-5} in our baseline models) and (2) that the Fe catalyzed conversion rate for formation of CH_3D, etc., is equal to the collision rate of the respective hydride with the Fe particles (i.e., the catalyst is 100% efficient). We note that both assumptions maximize production of the deuterated species. The collision time t_{coll} for production of a deuterated molecule such as NH_2D is then given by

$$t_{coll}(NH_2D) = [NH_2D]/[n_{Fe}\, v(2 \times 10^{-5})] , \qquad (26)$$

where n_{Fe} is the number density of (assumed monodisperse) Fe particles with radius r and v, which is the collision frequency of the respective hydride (NH_3 in this case) with the Fe particles is given by

$$v = 4.57 \times 10^4 [NH_3] T^{1/2} r_{Fe}^2 / M_{NH_3}^{1/2} . \qquad (27)$$

Equation (27) is simply the bimolecular collision frequency from the kinetic theory of gases with numerical constants

appropriate for collisions with Fe particles. Analogous expressions for other deuterated molecule collision times can be derived by substituting for NH_2D and NH_3 number densities and molecular weights where appropriate in equations (26) and (27). The quench temperatures corresponding to the collision times are then calculated in the usual fashion.

The resulting quench temperatures for NH_2D are illustrated in Figure 6 where they are also compared with the quench temperatures for homogeneous gas phase formation of NH_2D via equation (22). It is immediately apparent that if the Fe-catalyzed reactions are 100% efficient, then, at eddy diffusion coefficients $K > 2 \times 10^6$ cm^2 s^{-1}, deuterium exchange reactions may proceed to lower temperatures.

However, these results are only an upper limit to the catalyst efficiency and thus a lower limit to quench temperatures. A more realistic treatment of the Fe catalyst efficiency might be to assume that the efficiency for deuterium exchange is given by exp $(-E_a/RT)$, where E_a is the activation energy ($\sim$63 kJ mole^{-1}) for $NH_3 + D_2$ exchange on Fe metal. This efficiency is extremely small ($\sim 5 \times 10^{-4}$ at 1000 K falling to $\sim 3 \times 10^{-7}$ at 500 K). The resulting quench temperatures, which are also displayed in Figure 6, are thus always higher than the quench temperatures for the homogeneous gas phase reactions at all eddy diffusion coefficients less than $\sim 2 \times 10^{11}$ cm^2 s^{-1}. The results in Figure 6 are for 1 μm radius particles, but the same conclusion holds for all particles ($r \sim 0.8$–3 μm) which can be transported into this region of the atmosphere (Prinn and Olaguer 1981). Based on these calculations and buttressed by the fact that the presence of Fe-particle "clouds" in the deep atmospheres of Jupiter and Saturn is open to question (Fe may be sequestered in the core), we conclude that heterogeneous Fe catalysis does not alter the D/H ratios established by the homogeneous NH_3 gas phase reaction. Furthermore, even if such clouds are present we note that, except for NH_3, where Fe catalysis of deuterium exchange is well known (e.g., Farkas 1936; Gutmann 1953; Kemball 1952; Singleton, Roberts, and Winter 1951; Weber and Laidler 1951), there is little evidence for Fe catalysis of deuterium exchange for the molecules of interest (H_2O, CH_4, H_2S, etc.). Indeed, Fe is stated to be ineffective as a catalyst for deuterium exchange with CH_4 (Bond 1962) and H_2S is a catalyst poison for deuterium exchange (Singleton, Roberts, and Winter 1951).

We have also considered heterogeneous catalysis of deuterium exchange reactions by cloud particles and aerosols in the observable regions of the atmospheres of Jupiter and Saturn. Specifically, we have studied the possibility of catalysis by NH_4SH(s) cloud particles because the rotational temperatures determined from 4.7 μm observations of CH_3D on Jupiter

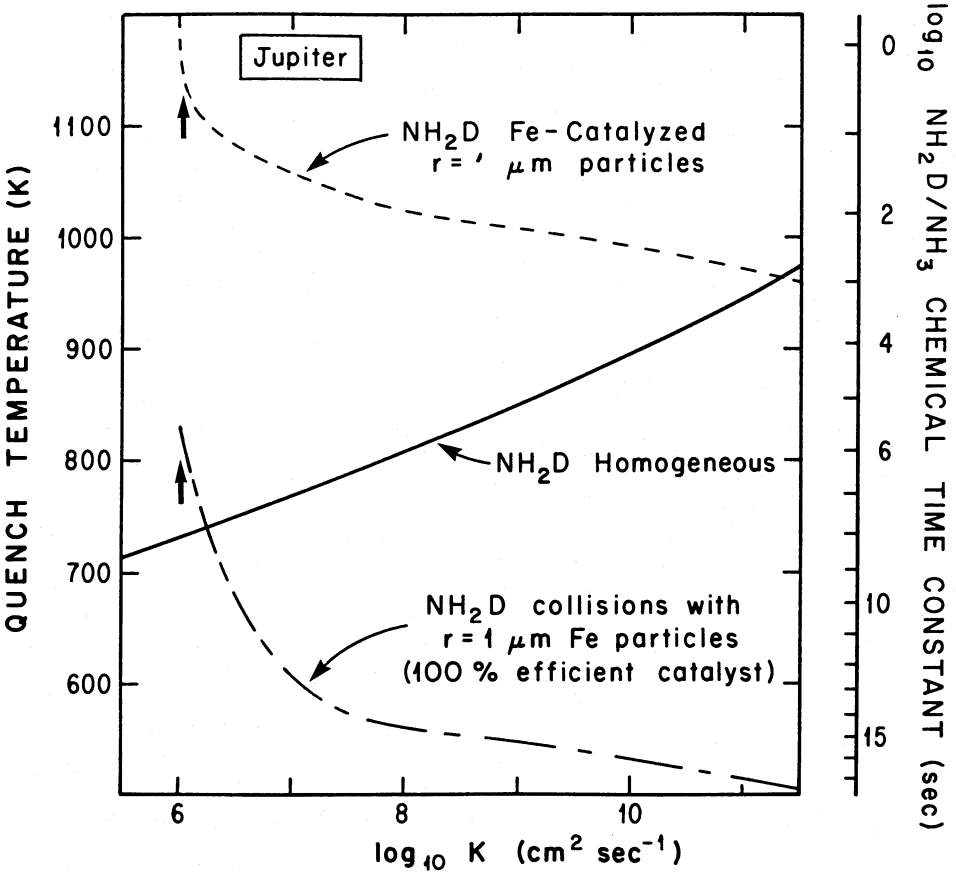

FIG. 6.—Comparison of homogeneous gas phase and heterogeneous Fe catalyzed deuterium exchange between NH_3 + HD in the atmosphere of Jupiter as a function of the vertical eddy diffusion coefficient K. The solid line is for the homogeneous gas phase reaction, the dash-dotted line is for heterogeneous catalysis where the collision frequency of NH_3 with $r = 1$ μm Fe particles is the rate determining step, and the short-dashed line is for heterogeneous catalysis with an efficiency equal to the efficiency of Fe for catalyzing the $NH_3 + D_2$ exchange. The method of Prinn and Olagauer (1981) was used to model Fe particle sizes and number densities as a function of altitude and vertical mixing rate in the deep atmosphere of Jupiter. The arrows show the point where $K = wH$ for particle sedimentation velocity w. Heterogeneous catalysis of deuterium exchange by Fe particles is predicted to be unimportant in the deep atmospheres of Jupiter and Saturn. Catalysis on cloud and aerosol particles is also predicted to be ineffective (*see text*).

(Beer and Taylor 1978*a*) and Saturn (Fink and Larson 1978) (220 ± 20 K and 175 ± 30 K, respectively) fall within the predicted stability field of NH_4SH clouds on these two planets (Lewis and Prinn 1984). Although we are unaware of any relevant experimental data, several independent lines of evidence suggest that heterogeneous catalysis by NH_4SH (and other types of cloud and aerosol particles) is ineffective for altering D/H ratios established by homogeneous gas phase reactions at deeper atmospheric levels.

First, model calculations assuming that NH_4SH is as efficient for catalyzing deuterium exchange reactions as Fe is show that heterogeneous catalysis is unimportant in this case. These calculations assume a temperature of 200 K, 100% condensation of H_2S as NH_4SH particles, and monodisperse spherical particle radii in the range of 1–10 μm. For 5 μm radius NH_4SH particles, the calculated t_{chem} for formation of NH_2D by NH_3 collisions on NH_4SH particles is then $\sim 10^{16}$ s versus $t_{conv} \sim 8 \times 10^8$ s if $K = 10^4$ cm^2 s^{-1}. This result is obviously not changed significantly if other particle radii are assumed or if catalysis by NH_3 particles at temperatures around 140 K is modeled instead. The inefficiency of particle catalysis is in accord with Singleton, Roberts, and Winter (1951) who demonstrated that the glass walls of their system did not catalyze deuterium exchange reactions between NH_3 and D_2. Furthermore, even if catalytic surfaces that are effective for some reactions (e.g., ortho-para H_2 conversion) were present, they would not necessarily catalyze deuterium exchange. For example, Harrison and McDowell (1953) found that the solid free radical α, α–diphenyl-β–picryl hydrazyl was effective for catalyzing ortho-para H_2 conversion at 90 K, but did not catalyze $H_2 + D_2$ exchange. In addition, Farkas (1936) showed that $NH_3 + D_2$ exchange is still slower; ortho-para H_2 conversion reactions and $H_2 + D_2$ exchange on an Fe catalyst can occur at temperatures 200 K lower than catalyzed $NH_3 + D_2$ exchange. Thus, there is no compelling reason to indicate that cloud and aerosol particles are catalytically altering D/H ratios in CH_3D (and other hydrides) that were established in the deep atmospheres of Jupiter and Saturn.

V. APPLICATIONS TO CH_3D OBSERVATIONS AND DERIVED D/H RATIOS

We have used the CH_3D fractionation factors in Table 3 to derive revised estimates of the D/H ratios for Jupiter and Saturn. Based on the CH_3D mixing ratios and C/H enrichments over solar given in Table 4 of Bjoraker, Larson, and Kunde (1986*a*) and the carbon solar abundance of Cameron (1982), equation (6) yields D/H $\sim (2.6 \pm 1.0) \times 10^{-5}$ for Jupiter. Similarly, the results of Fink and Larson (1978), Courtin *et al.* (1984), and DeBergh *et al.* (1986) for the CH_3D/CH_4 ratio on Saturn give D/H $\sim (1.7 \pm 1.0) \times 10^{-5}$ As noted previously by other authors, the mean D/H ratio for Saturn is apparently lower than the mean value for Jupiter. However, the derived D/H ratios for the two planets are identical within the uncertainty limits.

Several authors have noted that larger D/H ratios (in the range of 5×10^{-5}–1×10^{-4}) are derived for Jupiter and Saturn from observations of HD (e.g., see Bjoraker, Larson, and Kunde 1986*a*; Courtin *et al.* 1984; DeBergh *et al.* 1986). A comparison of the CH_3D and HD results for Jupiter is given in Figure 7, where constant CH_3D/CH_4 contours corresponding to D/H ratios of (1, 2, 5, and 10) $\times 10^{-5}$ are plotted. The contours are calculated from equation (6) using the baseline value of $\alpha = 1.205$ from Table 3. However, no noticeable

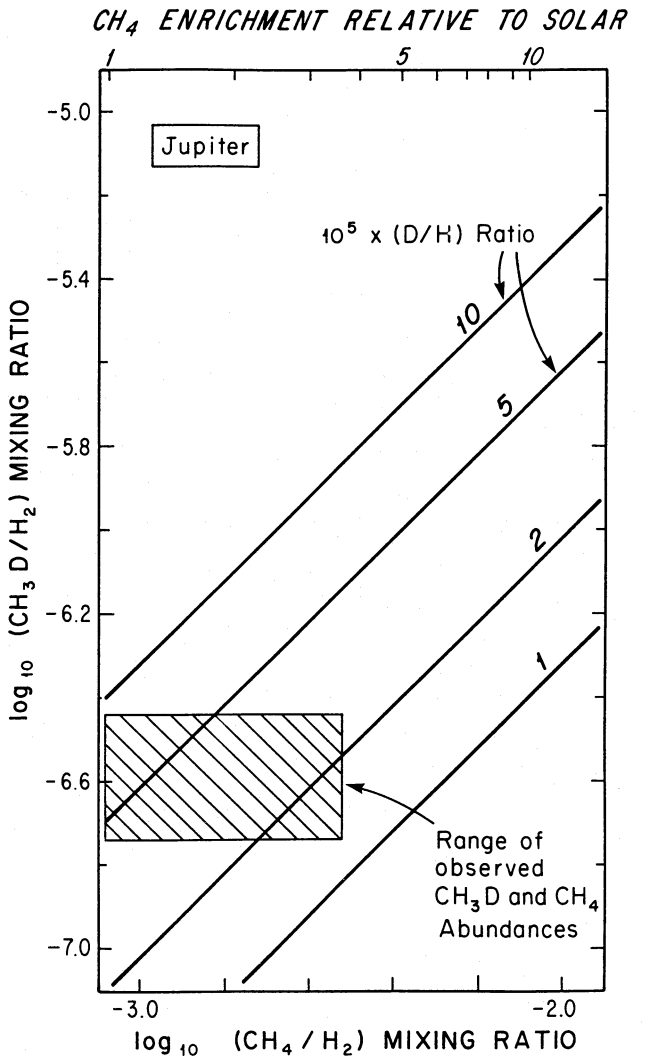

FIG. 7.— Comparison of the observed range of CH_3D and CH_4 mixing ratios in the atmosphere of Jupiter with constant contours of CH_3D/CH_4 corresponding to D/H atom ratios in the range of (1–10) $\times 10^{-5}$. D/H ratios of (5–10) $\times 10^{-5}$ are derived from observations of HD on Jupiter. More generally accepted CH_4/H_2 mixing ratios of ≥ 2.3 times solar result in D/H atom ratios below 4×10^{-5} and in apparent disagreement with the HD observations (*see text*).

changes in the contour positions occur for α values of 1.240–1.187 corresponding to eddy diffusion coefficients of 10^7–10^9 cm^2 s^{-1} required for heat transport by free convection in Jupiter's deep atmosphere. The range of observed CH_3D and CH_4 mixing ratios reported in the literature is also plotted; the CH_4 range is extended down to the solar CH_4/H_2 value.

Figure 7 illustrates that the observed range of CH_3D and CH_4 mixing ratios overlaps D/H ratios from $\sim 1.2 \times 10^{-5}$ to $\sim 9.0 \times 10^{-5}$ (for a solar CH_4/H_2 value). This overlap is reduced if we consider only recent CH_4 abundance determinations for Jupiter that indicate CH_4 enrichments relative to solar. For example, taking as a lower limit the *Voyager* IRIS CH_4/H_2 mixing ratio of 2.3 times the solar value (Gautier and Owen 1983; Gautier *et al.* 1982) reduces the intersection to D/H ratios of $\sim 1.2 \times 10^{-5}$–$\sim 4.0 \times 10^{-5}$.

There are two alternatives to explain the apparent differences between D/H ratios derived from the CH_3D and HD observations. First, the D/H ratios from the CH_3D observa-

tions are correct and the higher values derived from the HD observations are incorrect because of observational problems and/or difficulties in modeling line formation and radiative transfer for these weak lines in a cloudy atmosphere. Indeed, the ratios of adjacent HD, CH_4, and CH_3D line pairs determined by Encrenaz and Combes (1982) gave a D/H ratio of $(2.0^{+1.1}_{-0.8}) \times 10^{-5}$ for Jupiter, in agreement with the mean D/H ratio from the CH_3D observations given above.

The second alternative is that the D/H ratios derived from the HD observations are correct and the lower values from the CH_3D observations are incorrect. Several different circumstances may lead to this situation. First, CH_4 + HD may not equilibrate in the deep atmospheres of Jupiter and Saturn. However, although this explanation has been suggested by several authors, it is implausible because of the rapid chemical reaction rates at the high temperatures and pressures in the deep atmospheres of the two planets. For example, on Jupiter the chemical lifetime for CH_4 + HD equilibrium via reaction (17) is ~8 days at the predicted quench temperaure of 790 K and is only ~1 minute at 1000 K. A similar situation occurs on Saturn. Deuterium equilibration between CH_4 + HD will definitely occur under these conditions.

Another possible explanation is that equation (6) is giving anomalously low D/H ratios because of incorrect input parameters. This circumstance could result from an α value which is larger than it should be, an observed CH_3D/CH_4 ratio which is smaller than the equilibrium ratio at the quench temperature, or a combination of both factors. A comparison of two independent calculations of α values (Richet, Bottinga, and Javoy 1977; Burcat 1984) shows that uncertainties in α are only 5%–10%. This is too small to change the D/H ratio by the required factor of 2 to 4 times. Furthermore, α is constrained to be larger than unity. Thus, large decreases in the CH_3D/CH_4 ratio appear to be required. There is no mechanism for increasing the amount of CH_4 in the observable regions of the atmospheres of Jupiter and Saturn relative to the amount in the deep atmosphere. However, there are also very few plausible mechanisms for decreasing the amount of CH_3D in the visible regions relative to that in the deep atmosphere. Heterogeneous catalysis on the surfaces of cloud and aerosol particles is one possibility. However, even if effective, which is probably not the case as shown above, heterogeneous catalysis would have the opposite effect of increasing CH_3D. Loss of CH_3D by solution in the predicted aqueous solution clouds (Lewis and Prinn 1984) is another possibility. But a calculation intentionally neglecting any CH_4 solubility (thus giving an estimate of the *maximum* possible CH_3D/CH_4 decrease) and assuming the same Henry's law constant as CH_4 (Wagman *et al.* 1968) shows that only $\sim 2 \times 10^{-5}$ of the available CH_3D will dissolve in the clouds ($T \sim 300$ K).

The isotopically selective destruction of CH_3D relative to CH_4 is also a possibility. The mass difference between CH_3D and CH_4 and the different molecular symmetries (C_{3v} vs. T_d) will lead to different vibrational and rotational frequencies and transition rules. As a result, transitions between discrete states will occur at different frequencies. For example, Hsu and Manuccia (1980) have demonstrated isotopically selective destruction of CH_3D relative to CH_4 via reaction of vibrationally excited CH_3D with Br atoms. However, the required CO_2 laser energy source is obviously not present in the atmospheres of Jupiter and Saturn. On the other hand, various natural processes may lead to the preferential destruction of only one or a few of the isotopic forms of a particular molecule. For example, Cicerone and McCrumb (1980) suggested that isotopic self-shielding of $^{16}O_2$ in the Schumann-Runge (S-R) absorption bands could lead to the preferential photolysis of $^{18}O^{16}O$ at levels where $^{16}O_2$ has reached a large optical depth in the S-R bands. Isotopically heavy $^{50}O_3$ has subsequently been observed (Mauersberger 1987; Rinsland *et al.* 1985) in amounts over those which would be present statistically, although the self-shielding appears inadequate to account for the observed enhancement (Blake, Gibson, and McCoy 1984; Kaye 1987). However, CH_4 displays only continuum absorption in the region where photolysis occurs, so isotopic self-shielding of absorption lines is not possible. Another isotopically selective mechanism is the preferential absorption by one isotopic species of the strong emission line of a natural source. For example, this occurs for H Lyα absorption by the $^{12}C^{16}O$ form of CO (Arrhenius, Corrigan, and Fitzgerald 1980). The data of Laufer and McNesby (1965) indicate that the CD_4 absorption coefficient is ~30% larger than the CH_4 absorption coefficient at 1216 Å (H Lyα line), where most CH_4 photolysis occurs. However, a smaller effect is expected for CH_3D, and, in any case, a decrease in the CH_3D/CH_4 ratio by a factor of 2 to 4 (not just by 30%) is required. Finally, preferential $^{12}C^{16}O$ dissociation can also occur because near coincidences with several H_2 absorption lines shield the other isotopic CO species (Glassgold, Huggins, and Langer 1985), although we are unaware of a similar occurrence for CH_4 and CH_3D. However, the isotopically selective destruction of CH_3D relative to CH_4 in the visible regions of the atmospheres of Jupiter and Saturn by differences in the rates of the nonphotolytic reactions (e.g., isotopic exchange reactions) involved in CH_3D and CH_4 photochemistry at high altitude cannot be unambiguously ruled out until suitably detailed photochemical calculations of the type reviewed elsewhere (Atreya and Romani 1985; Kaye 1987; Strobel 1985) are performed.

This exhaustive examination of possible explanations for the apparent discrepancy between D/H ratios derived from CH_3D and HD observations leads us to conclude that the first alternative of incorrect D/H values from the HD observations is the most likely solution. Two different approaches may prove useful for resolving this apparent paradox. First, the observation of HD in the submillimeter region as proposed by Bezard, Gautier, and Marten (1986) will give an independent estimate of the HD/H_2 ratios on Jupiter and Saturn. Second, the observation of other deuterated hydrides such as HDO and NH_2D will give independent estimates of the D/H ratio from deuterium exchange reactions via equations (7)–(8) and the respective fractionation factors in Table 3. However, at present, the exact D/H ratios on Jupiter (e.g., see Fig. 7) and Saturn are effectively unconstrained within a wide range.

VI. ISOTOPIC EXCHANGE REACTIONS FOR NONEQUILIBRIUM TRACE GASES (CO, CO_2, N_2, HCN)

Isotopic exchange reactions in the atmospheres of Jupiter and Saturn are not limited to reactions involving deuterium, but also occur for all elements with more than one stable isotope and present in more than one chemical reservoir. This is the case for carbon, nitrogen, and oxygen. The less abundant $^{13}CH_4$ form of methane has been observed on both Jupiter (Fox *et al.* 1972; Courtin *et al.* 1983 and references therein) and Saturn (Combes, Maillard, and DeBergh 1977) although the *Voyager* IRIS $^{12}C/^{13}C$ ratio of 160^{+40}_{-55} is significantly larger than the lower values (~90) obtained from ground-based observations. Drossart *et al.* (1985) have also observed

$^{13}C^{12}CH_2$ on Jupiter at a $^{13}C\,^{12}CH_2/^{12}C_2H_2$ ratio of 20^{+20}_{-10}, which they interpreted as a photochemical fractionation effect. There are also several observations of $^{15}NH_3$ on Jupiter (Lacy *et al.* 1975; Encrenaz, Combes, and Zeau 1978; Tokunaga *et al.* 1979; Drossart, Encrenaz, and Combes 1985), but the derived $^{14}N/^{15}N$ ratios vary from solar ($\sim$272) to $\sim$125. There are no observations of $^{15}NH_3$ on Saturn or of $H_2^{18}O$ on either Jupiter or Saturn. Furthermore, these are presently no observations of isotopic fractionation between various trace gases which are presumably mixed upward from the deep atmosphere (e.g., $^{13}C/^{12}C$ in CO and HCN). However, such isotopic fractionations are potentially very useful for discriminating between photochemical sources in the upper atmospheres and thermochemical sources in the lower atmospheres for nonequilibrium trace gases such as CO, HCN, N_2, and CO_2. The predicted $^{13}C/^{12}C$, $^{15}N/^{14}N$, and $^{18}O/^{16}O$ fractionations resulting from thermochemical equilibrium between these trace gases and the major reservoirs (CH_4, NH_3, H_2O) are calculated below.

The exchange of C, N, and O isotopes via the equilibria

$$^{13}CH_4 + {}^{12}CO = {}^{12}CH_4 + {}^{13}CO\,, \quad (28)$$

$$^{13}CH_4 + {}^{12}CO_2 = {}^{12}CH_4 + {}^{13}CO_2\,, \quad (29)$$

$$^{13}CH_4 + H{}^{12}CN = {}^{12}CH_4 + H\,{}^{13}CN\,, \quad (30)$$

$$^{15}NH_3 + \tfrac{1}{2}{}^{14}N_2 = {}^{14}NH_3 + \tfrac{1}{2}{}^{15}N_2\,, \quad (31)$$

$$^{15}NH_3 + HC^{14}N = {}^{14}NH_3 + HC^{15}N\,, \quad (32)$$

$$H_2{}^{18}O + C^{16}O = H_2{}^{16}O + C^{18}O\,, \quad (33)$$

$$H_2^{18}O + \tfrac{1}{2}C^{16}O_2 = H_2^{16}O + \tfrac{1}{2}C^{18}O_2\,. \quad (34)$$

For the less abundant ^{17}O isotope, the differences for the $^{17}O/^{16}O$ and $^{18}O/^{17}O$ ratios between H_2O and CO and CO_2 will be approximately half the difference in the $^{18}O/^{16}O$ ratio. The equilibrium constants for reactions (28)–(34) can be expressed in terms of isotopic fractionation factors defined following the convention previously used for deuterium. These fractionation factors, which are tabulated in several places (e.g., Richet, Bottinga, and Javoy 1977; Urey 1947), vary as a function of temperature. However, the smaller mass ratios between the isotopes involved lead to smaller α values than obtained for D/H exchange.

The elementary reactions and rate-determining steps responsible for quenching the C, N, and O isotopic fractionations in equilibria (28)–(34) are assumed to be the same as those responsible for quenching the concentrations of CO, HCN, N_2, and CO_2. The relevant kinetics and rate constants have been discussed previously (Prinn and Barshay 1977; Prinn and Olaguer 1981; Fegley and Prinn 1985, 1986). Note that in this first-order treatment we are neglecting any kinetic isotope effects which are likely to be small at high ($T \sim 1000$ K) temperatures. The results of our calculations, which are presented in Table 4 and Figures 8 and 9, illustrate several important points.

First, all of the predicted fractionation factors are in the same range as observed isotopic fractionations for many terrestrial processes. For example, Table 4 shows that the predicted $^{13}C/^{12}C$ ratio in CO is 3 parts per 1000 smaller than the $^{13}C/^{12}C$ ratio in CH_4 at a CO quench temperature of 1065 K on Jupiter. We note that the fractionation factors for $^{13}C/^{12}C$, $^{15}N/^{14}N$, $^{18}O/^{16}O$, etc., are not dependent on the actual isotopic ratios on Jupiter and Saturn. In fact, expressions similar to equations (6)–(9) for the D/H atom ratios on Jupiter and Saturn can also be written for the $^{13}C/^{12}C$, etc., atom ratios if so desired. However, this does not appear necessary at the present time because the required accuracy and precision are not available from remote sensing techniques, although informative measurements could be made by a suitably designed mass spectrometer on an entry probe.

Our results also predict that relative to CH_4, CO_2 will contain more ^{13}C, while CO will contain less ^{13}C. The predicted $^{13}C/^{12}C$ fractionations in CO_2 on Jupiter and Saturn are also generally larger than those predicted for CO. However, both CO_2 and CO are predicted to be enriched in ^{18}O relative to H_2O by 3–4 parts per 1000. Finally, both HCN and N_2 are predicted to have smaller $^{15}N/^{14}N$ ratios than NH_3 by 2 parts per 1000. All of these fractionations would be resolvable in terrestrial samples.

The quantitative calculation of predicted isotopic ratios for photochemically produced CO, CO_2, N_2, and HCN is beyond

TABLE 4

PREDICTED FRACTIONATION FACTORS FOR $^{13}C/^{12}C$, $^{15}N/^{14}N$, AND $^{18}O/^{16}O$ EXCHANGE ON JUPITER AND SATURN

	JUPITER[a]			SATURN[a]		
GAS	Quench Temperature[b] (K)	Fractionation Factor[c] (α)	Predicted Mixing Ratio	Quench Temperature[b] (K)	Fractionation Factor[c] (α)	Predicted Mixing Ratio
CO[c]	1065	0.997 1.004[d]	1.9×10^{-9}	980	0.997 1.004[d]	1.3×10^{-10}
CO_2[c]	1020	1.008 1.003[d]	2.8×10^{-12}	960	1.010 1.004[d]	4.2×10^{-13}
HCN[c]	1510	1.001 0.998[e]	1.4×10^{-9}	1430	1.001 0.998[e]	1.7×10^{-10}
N_2	1655	0.998	1.0×10^{-5}	1580[f]	0.998	2.5×10^{-6}

[a] Predictions assume 2.3 times solar composition for Jupiter, 2.5 times for Saturn, and $K_{eddy} = 2 \times 10^8$ cm^2 s^{-1} for both planets.

[b] For homogeneous gas phase reaction only.

[c] $\alpha = [(^{13}C/^{12}C)\text{gas}]/[(^{13}C/^{12}C)\text{methane}]$.

[d] $\alpha = [(^{18}O/^{16}O)\text{gas}]/[(^{18}O/^{16}O)\text{water}]$.

[e] $\alpha = [(^{15}N/^{14}N)\text{gas}]/[(^{15}N/^{14}N)\text{ammonia}]$.

[f] The quench temperature of 1380 K for homogeneous gas phase destruction of N_2 given in Table 1 of Fegley and Prinn 1985 is a typographical error.

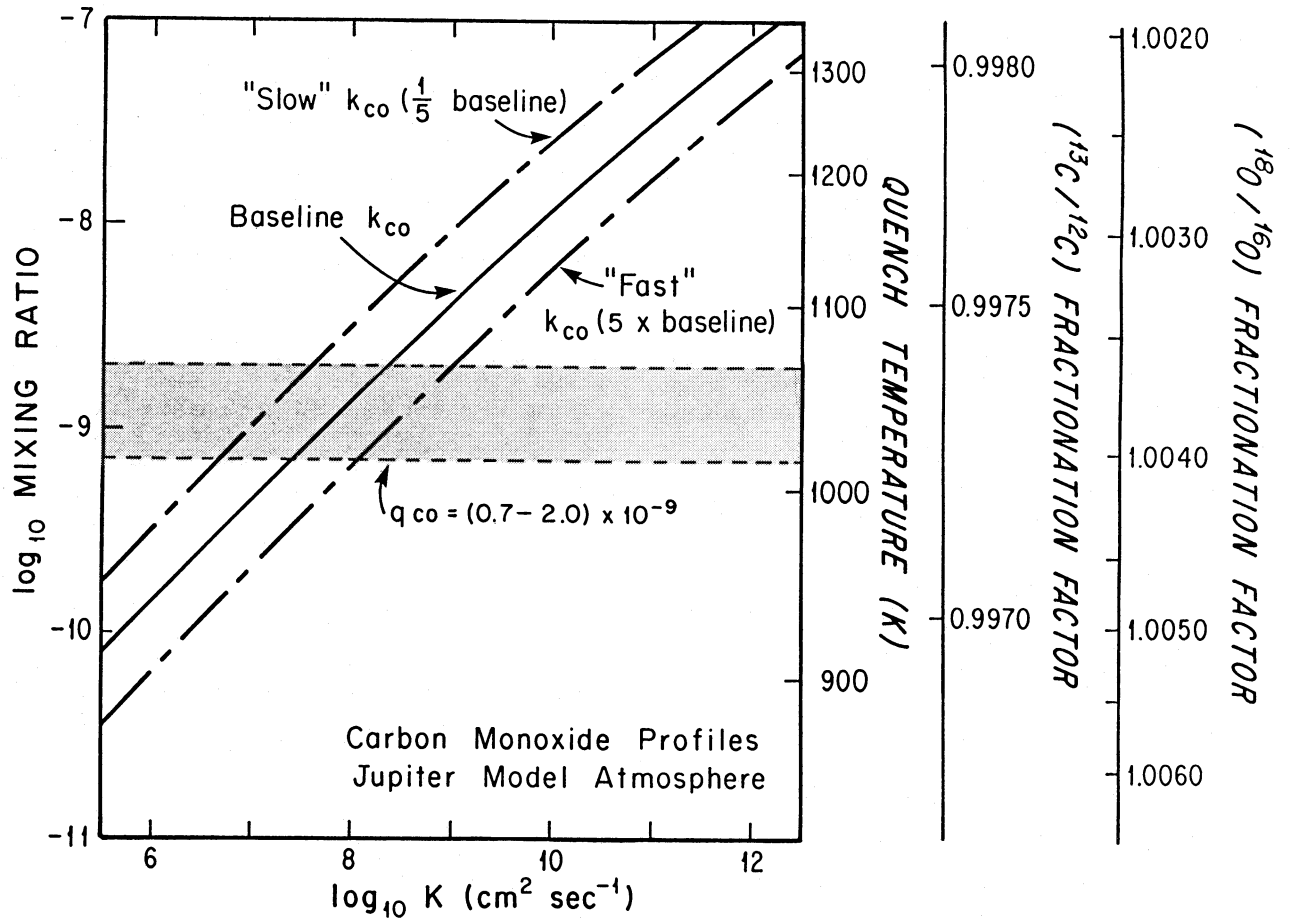

FIG. 8.—Predicted CO mixing ratios in the visible Jovian atmosphere as a function of the vertical eddy diffusion coefficient K. The vertical scales show the predicted $^{13}C/^{12}C$ and $^{18}O/^{16}O$ fractionation factors for isotopic exchange with CH_4 and H_2O, respectively, as a function of the CO quench temperature. The shaded region shows the range of CO mixing ratios reported in the literature (Beer and Taylor 1978*b*; Larson *et al.* 1978; Bjoraker, Larson, and Kunde 1986*a*; Noll *et al.* 1988). The solid curve utilizes the baseline rate constant for CO destruction from Prinn and Barshay (1977) and the two dashed lines show the effects of uncertainties of a factor of 5 in this rate constant. The predicted CO mixing ratio is consistent with the observed value within the expected uncertainties in the rate constant and the vertical eddy diffusion coefficient.

the scope of this work. However, a variety of factors suggest that the photochemical isotopic ratios may be quite different from the thermochemical isotopic ratios. First, kinetic isotope effects and fractionation factors will be larger at stratospheric temperatures ($T \sim 100$–160 K) than at quench temperatures of $\sim$1000 K. Second, isotopic self-shielding may occur for $^{14}NH_3$, leading to enhanced photolysis rates for $^{15}NH_3$ if the isotopic line shifts are greater than the $^{14}NH_3$ line widths. A similar effect for $^{14}NH_3$ and $^{14}NH_2D$ may produce distinctive D/H ratios in photochemically produced HCN. Third, the isotopic composition of the photolysis products may also be altered selectively by photochemical processes (e.g., the selective photodecomposition of $^{12}C^{16}O$ mentioned earlier). In any case we emphasize that the photochemical production of CO on Jupiter remains speculative because the most recent observational data indicate rotational temperatures and pressure-broadened line widths consistent with a tropospheric distribution (Bjoraker, Larson, and Kunde 1986*a*; Noll *et al.* 1988).

Figure 8 shows updated results for the predicted CO mixing ratios in the visible Jovian atmosphere as a function of the vertical eddy diffusion coefficient K. These calculations, which utilize the 2.3 times solar baseline model for Jupiter's atmosphere, predict a CO mixing ratio of 1.9×10^{-9} for $K = 2 \times 10^8$ cm^2 s^{-1} in agreement with the observed CO mixing ratio of $\sim(0.7–2.0) \times 10^{-9}$ (Larson, Fink, and Treffers 1978; Beer and Taylor 1978*b*; Bjoraker, Larson, and Kunde 1986*a*; Noll *et al.* 1988). Figure 8 also shows the effects of our estimated uncertainties in the rate coefficient for CO destruction (Prinn and Barshay 1977) on the predicted CO mixing ratios. These calculations show that, within the range of permissible eddy diffusion coefficients (10^7 to 10^9 cm^2 s^{-1}), factor of 5 changes in the rate constant still lead to agreement with the observed CO mixing ratio.

Finally, Figure 9 displays predicted HCN mixing ratios and $^{13}C/^{12}C$ isotopic ratios as a function of quench temperatures over a wide range of vertical eddy diffusion coefficients. This is the first quantitative treatment of HCN thermochemical kinetics on Jupiter and utilizes all the HCN destruction reactions for which kinetic data are available (summarized by Fegley *et al.* 1986). In agreement with our previous work (Prinn and Fegley 1981; Fegley and Prinn 1985) we find that reaction of HCN with H_2 is the rate-determining step. Lewis and Fegley (1984) previously discussed HCN quenching on Jupiter but did not do quantitative calculations.

Table 4 and Figure 9 show that, contrary to popular belief,

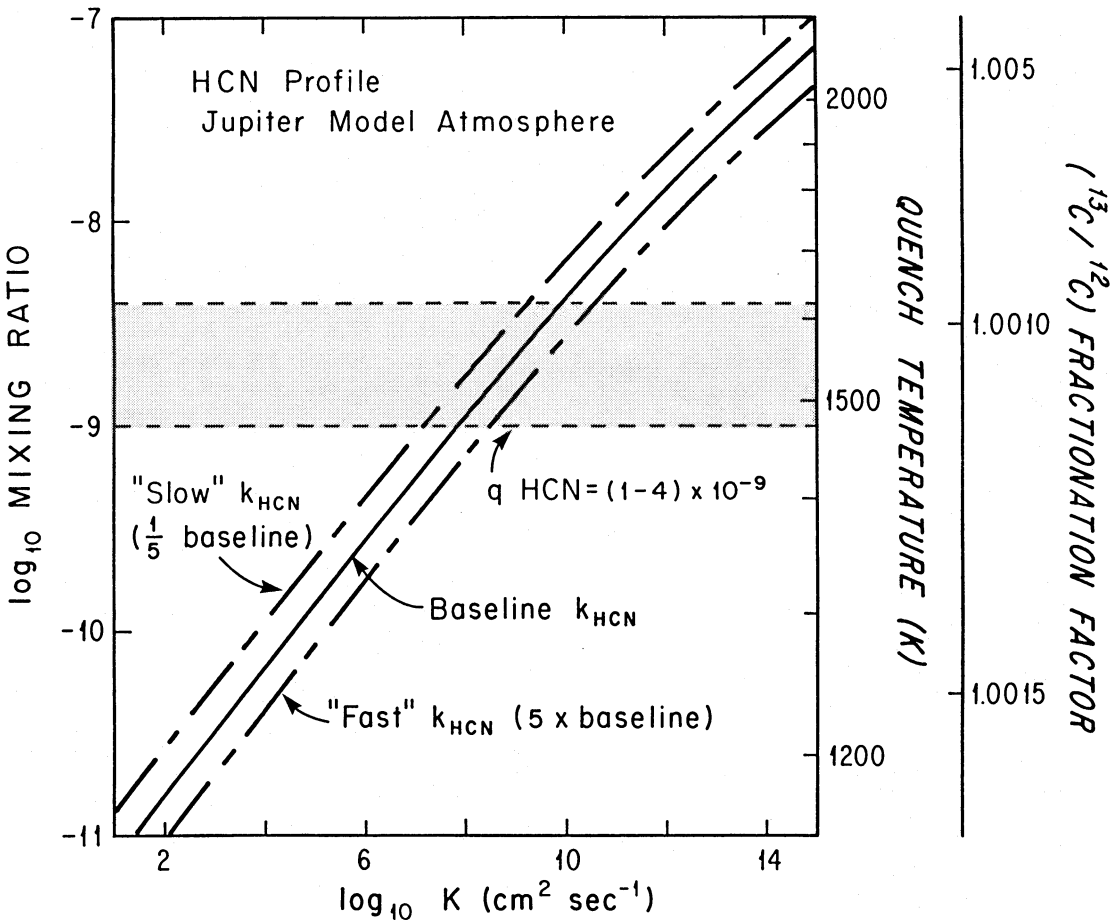

FIG. 9.—As in Fig. 8 but for HCN. Only the $^{13}C/^{12}C$ fractionation factor is shown because the $^{15}N/^{14}N$ fractionation factor = 0.998 throughout the temperature range shown. The range of observed HCN mixing ratios is from Tokunaga *et al.* (1981). The predicted HCN mixing ratio is consistent with the observed value within the expected uncertainties in the rate constant and the vertical eddy diffusion coefficient.

vertical transport of HCN from Jupiter's deep atmosphere provides a HCN mixing ratio of $\sim 10^{-9}$, consistent with the observed HCN abundance of $\sim(1\text{–}4) \times 10^{-9}$ (Tokunaga *et al.* 1981). Furthermore, Figure 9 also shows that, like CO, the acceptable range of eddy diffusion coefficients permits substantial variations in the rate constant (Prinn and Fegley 1981). Lightning and photochemistry have also been suggested as possible sources for the HCN observed on Jupiter. However, as reviewed by Lewis and Fegley (1984), an absolute upper limit on the lightning-produced HCN mixing ratio is $\sim 3 \times 10^{-12}$ (assuming 100% of Jupiter's internal heat flux is converted into lightning at 100% efficiency), which is ~300–1300 times smaller than the observed mixing ratio of $\sim(1\text{–}4) \times 10^{-9}$. Photochemical production of HCN is more plausible but depends on estimates of several unknown rate constants and branching ratios and requires slow vertical mixing ($K \sim 10^4$ cm^2 s^{-1}) above the ammonia clouds (Kaye and Strobel 1983). The ability of vertical mixing to provide the entire observed HCN abundance implies that reactions responsible for HCN production via photochemistry possibly proceed slower (and may be less important) than estimated by Kaye and Strobel (1983). However, an unambiguous assessment of the relative importance of the photochemical and thermochemical sources for HCN is not possible at present. In any case, the results in Table 4 and Figure 9 are consistent with our prior conclusions that vertical mixing provides the dominant contribution to tropospheric HCN on both Jupiter and Saturn (Fegley and Prinn 1985).

VII. ISOTOPIC FRACTIONATION DURING THE CONDENSATION OF CLOUD-FORMING MATERIALS

The formation of condensation clouds such as aqueous solution, water ice, NH_4SH(s), and NH_3(s) clouds on Jupiter and Saturn will also alter the isotopic ratios (e.g., D/H, $^{15}N/^{14}N$, $^{18}O/^{16}O$, $^{34}S/^{32}S$) in the cloud particles (or droplets) and the residual vapor. These effects will only be mentioned briefly because their complete consideration is beyond the scope of this paper. However, isotopic variations between cloud particles and vapor are diagnostic of the physical processes involved in cloud formation (e.g., see Gat 1980; Dansgaard 1964). Furthermore, the isotopic variations are potentially detectable by a suitably designed mass spectrometer on an entry probe or on a balloon. We note that entry probes on Venus have provided data from the 90 bar, 750 K surface and that instrumented balloons have also been used to study the Venus atmosphere. In fact, Donahue *et al.* (1982) derived a D/H ratio for Venus from the analysis of a cloud droplet in the *Pioneer* Venus large-probe mass spectrometer. Thus, a brief discussion is worthwhile, and will aid in the design of future spacecraft experiments.

Isotopic exchange during condensation processes occurs by

reactions such as

$$HDO(g) + H_2O(s, l) = H_2O(g) + HDO(s, l) , \quad (35)$$

$$H_2{}^{18}O(g) + H_2{}^{16}O(s, l) = H_2{}^{16}O(g) + H_2{}^{18}O(s, l) , \quad (36)$$

$$NH_2D(g) + NH_3(s) = NH_3(g) + NH_2D(s) , \quad (37)$$

with equilibrium constants given by the ratios of the vapor pressures of the different isotopic species. These can be written in terms of fractionation factors defined as shown below for D/H:

$$\alpha(\text{ice/gas}) = [(D/H)_{ice}]/[(D/H)_{gas}] . \quad (38)$$

Functional fits to the appropriate fractionation factors (Friedman and O'Neil 1977; Jansco and Van Hook 1974; Kirshenbaum and Urey 1942) for reactions (35) and (36) at ~230–300 K and for reaction (37) below 195 K are

$$\log_{10} \alpha_{35}(\text{ice/gas}) = -0.04071 + 7045.414/T^2 , \quad (39)$$

$$\log_{10} \alpha_{35}(\text{liquid/gas}) = -0.040 + 6276.196/T^2 , \quad (40)$$

$$\log_{10} \alpha_{36}(\text{ice/gas}) = -1.927 \times 10^{-3} + 637.312/T^2 , \quad (41)$$

$$\log_{10} \alpha_{36}(\text{liquid/gas}) = -8.92 \times 10^{-4} + 437.591/T^2 , \quad (42)$$

$$\log_{10} \alpha_{37}(\text{solid/gas}) = -0.044 + 16.56/T , \quad (43)$$

where the subscripts refer to reactions (35)–(37) and the NH_2D vapor pressure is estimated via the relation

$$P_{NH_2D} \sim (P_{NH_3}/P_{ND_3})^{1/3} \quad (44)$$

from Kirshenbaum and Urey (1942).

Conventional models for the formation of condensation clouds on Jupiter and Saturn (e.g., Lewis and Prinn 1984) assume that equilibrium conditions prevail and the condensed phase is removed from the upwelling gas parcel. Under these conditions, the isotopic fractionation between a condensible species in the vapor and the condensed phase is described by the Rayleigh distillation equations

$$R_l/R_{l_0} = f^{(1-\alpha)} , \quad (45)$$

$$R_v/R_{v_0} = f^{(1-1/\alpha)} \sim f^{(\alpha-1)} , \quad (46)$$

where R_i is the isotopic ratio in phase i, l is liquid, v is vapor, subscript 0 refers to initial conditions, f is the fraction of liquid left with $1 \geq f > 0$, and α is the temperature-dependent fractionation factor. Equation (45) can also be applied to solid cloud particles. Gat (1980) and Dansgaard (1964) describe how equations (45) and (46) and more complex variants can be used to model isotopic fractionation in the terrestrial water cycle. We merely note that the conventional model for condensation cloud formation on Jupiter and Saturn leads to predictable variations in the D and ^{18}O isotopic compositions of cloud droplets and vapor given by

$$E_{D_v}/E_{18O_v} \sim E_{D_l}/E_{18O_l} \sim (1 - \alpha_D)/(1 - \alpha_{18O}) , \quad (47)$$

where $E_i = R/R_0 - 1$ is the phase enrichment. The ratio of E_D/E_{18O} is ~9.3 at 273 K and increases as temperature decreases.

VIII. CONCLUDING REMARKS

The results of our thermochemical equilibrium calculations predict that, in addition to HD and CH_3D which have already been observed, the most abundant deuterium-bearing gases in the atmospheres of Jupiter and Saturn are HDO (below the aqueous solution/water ice cloud base), NH_2D, and HDS. Several other deuterium-bearing gases are also predicted to be present with volume mixing ratios $\leq 10^{-9}$; these include PH_2D, DCl, CH_2D_2, DF, and D_2O. Given the observed low H_2O mixing ratios on Jupiter and the stringent upper limits on H_2S abundances in the visible atmospheres of Jupiter and Saturn, NH_2D is perhaps the best candidate for detection by remote sensing.

The abundances of the deuterium-bearing gases increase with decreasing temperature. We have studied quantitatively the quenching of deuterium exchange reactions for CH_3D, HDO, NH_2D, DCl, DF, and DCN using kinetic data from the literature and methods previously applied to the quenching of nonequilibrium trace gases such as CO, PH_3, GeH_4, and N_2 (Fegley and Prinn 1985). The resulting quench temperatures for these deuterium-bearing gases are in the range of 700–1000 K. These quench temperatures and the respective fractionation factors for D/H exchange are independent of the assumed elemental composition and D/H ratio. Our results for CH_3D fractionation factors on Jupiter differ importantly from those of Beer and Taylor (1973, 1978*a*). Thus, these gases are isotopic probes of the deep atmospheres of Jupiter and Saturn and sample atmospheric regions intermediate between those probed by CO, PH_3, GeH_4, and N_2 ($T \sim 1000$–1600 K) and those probed by ortho-para transitions in H_2 ($T \sim 130$–160 K; Massie and Hunten 1982; Conrath and Gierasch 1984). Furthermore, a quantitative study of possible heterogeneous surface-catalyzed reactions on putative Fe grains and on observed cloud particles shows that heterogeneous catalysis is unimportant for deuterium exchange reactions.

Analogous treatment of $^{13}C/^{12}C$, $^{15}N/^{14}N$, and $^{18}O/^{16}O$ isotopic fractionation between nonequilibrium trace gases (CO, CO_2, N_2, HCN) and the major chemical reservoirs (CH_4, H_2O, NH_3) for C, O, and N suggests that isotopic ratios in the trace gases can distinguish, in principle, between photochemical sources in the upper atmospheres and thermochemical sources in the lower atmospheres. However, the observed CO and HCN abundances on Jupiter are consistent with vertical transport of these species from the deep atmosphere. We have noted previously that the major source of tropospheric N_2 on Jupiter and Saturn is expected to be vertical transport from the deep atmospheres (Prinn and Olaguer 1981; Fegley and Prinn 1985).

Finally, we have examined in detail the possible processes responsible for the apparent discrepancies between D/H ratios derived from observations of HD and CH_3D on Jupiter and Saturn. The popular explanation invoking a failure for CH_4 + HD to equilibrate in the deep atmospheres is not tenable because the equilibrium time constant is ~8 days at predicted CH_3D quench temperatures and ~1 minute at 1000 K. Several other possible processes for altering the CH_3D/CH_4 ratio, including isotopically selective photolysis of CH_3D in the visible atmospheres of Jupiter and Saturn, do not appear able to resolve the apparent discrepancy. One mechanism which has yet to be quantitatively addressed is possible CH_3D depletion due to the small differences in nonphotolytic reaction rates for CH_3D and CH_4. With this caveat we conclude from our current knowledge that the D/H ratios derived from the HD observations are probably incorrect. This conclusion is supported by results of Encrenaz and Combes (1982) who determined ratios for adjacent line pairs of HD, CH_4, and CH_3D and obtained a D/H ratio in agreement with that derived from observations of CH_3D. Observations of HD in

the submillimeter region (Bezard, Gautier, and Marten 1986) and of HDO and NH_2D should resolve these discrepancies.

This work was supported by NASA grant NAGW-997 and NSF grant ATM-8710102 to MIT. We thank C. Maeda and A. Nash for assisting with coding while working in the MIT UROP program, D. Souza for drafting the figures, and G. Rodriguez for becoming a (novice) $T_EX$nician.

REFERENCES

Arrhenius, G., Corrigan, M. J., and Fitzgerald, R. W. 1980, *Lunar Planet. Sci.*, **11**, 34.
Atreya, S. K., and Romani, P. N. 1985, in *Recent Advances in Planetary Meteorology*, ed. G. E. Hunt (Cambridge: Cambridge University Press), p. 17.
Barshay, S. S., and Lewis, J. S. 1978, *Icarus*, **33**, 593.
Baulch, D. L., Cox, R. A., Hampson, R. F., Jr., Kerr, J. A., Troe, J., and Watson, R. T. 1984, *J. Phys. Chem. Ref. Data*, **13**, 1259.
Baulch, D. L., Drysdale, D. D., Duxbury, J., and Grant, S. J. 1976, *Evaluated Kinetic Data for High Temperature Reactions*, Vol. **3** (London: Butterworths).
Baulch, D. L., Duxbury, J., Grant, S. J., and Montague, D. C. 1981, *Evaluated Kinetic Data for High Temperature Reactions*, Vol. **4** (London: Butterworths) (*J. Phys. Chem. Ref. Data*, Vol. **10**, Suppl. No. 1 [1981]).
Beer, R., and Taylor, F. W. 1973, *Ap. J.*, **179**, 309.
———. 1978*a*, *Ap. J.*, **219**, 763.
———. 1978*b*, *Ap. J.*, **221**, 1100.
Bezard, B., Gautier, D., and Marten, A. 1986, *Astr. Ap.*, **161**, 387.
Bjoraker, G. L., Larson, H. P., and Kunde, V. G. 1986*a*, *Icarus*, **66**, 579.
———. 1986*b*, *Ap. J.*, **311**, 1058.
Black, D. C. 1973, *Icarus*, **19**, 154.
Blake, A. J., Gibson, S. T., and McCoy, D. G. 1984, *J. Geophys. Res.*, **89**, 7277.
Bond, G. C. 1962, *Catalysis by Metals* (London: Academic Press).
Bottinga, Y. 1969, *Geochim. Cosmochim. Acta*, **33**, 49.
Burcat, A. 1980, *Ideal Gas Thermodynamic Functions of Hydrides and Deuterides*, Report TAE No. 411 (Haifa: Technion Israel Institute of Technology).
Burcat, A. 1984, in *Combustion Chemistry*, ed. W. C. Gardiner, Jr. (New York: Springer Verlag), p. 455.
Cameron, A. G. W. 1973, *Space Sci. Rev.*, **15**, 121.
———. 1982, in *Essays in Nuclear Astrophysics*, ed. C. A. Barnes, D. D. Clayton, and D. N. Schramm (Cambridge: Cambridge University Press), p. 23.
Chase, M. W., Jr., Davies, C. A., Downey, J. R., Jr., Frurip, D. J., McDonald, R. A., and Syverud, A. N. 1985, *J. Phys. Chem. Ref. Data, JANAF Thermochemical Tables* (3d ed.), **14**, Suppl. No. 1.
Cicerone, R. J., and McCrumb, J. L. 1980, *Geophys. Res. Letters*, **7**, 251.
Combes, M., Maillard, J. P., and DeBergh, C. 1977, *Astr. Ap.*, **61**, 531.
Courtin, R., Gautier, D., Marten, A., and Kunde, V. 1983, *Icarus*, **53**, 121.
Courtin, R., Gautier, D., Marten, A., Bezard, B., and Hanel, R. 1984, *Ap. J.*, **287**, 899.
Conrath, B. J., Gautier, D., Hanel, R. A., and Hornstein, J. S. 1984, *Ap. J.*, **282**, 807.
Conrath, B. J., and Gierasch, P. J. 1984, *Icarus*, **57**, 184.
Dansgaard, W. 1964, *Tellus*, **16**, 436.
DeBergh, C., Lutz, B. L., Owen, T., Brault, J., and Chauville, J. 1986, *Ap. J.*, **311**, 501.
Donahue, T. M., Hoffman, J. H., Hodges, R. R., Jr., and Watson, A. J. 1982, *Science*, **216**, 630.
Drossart, P., Encrenaz, T., and Combes, M. 1985, *Astr. Ap.*, **146**, 181.
Drossart, P., Encrenaz, T., Kunde, V., Hanel, R., and Combes, M. 1982, *Icarus*, **49**, 416.
Drossart, P., Lacy, J., Serabyn, E., Tokunaga, A., Bezard, B., and Encrenaz, T. 1985, *Astr. Ap.*, **149**, L10.
Encrenaz, T., and Combes, M. 1982, *Icarus*, **52**, 54.
Encrenaz, T., Combes, M., and Zeau, Y. 1978, *Astr. Ap.*, **70**, 29.
Farkas, A. 1936, *Trans. Faraday Soc.*, **32**, 416.
Fegley, B., Jr., and Lewis, J. S. 1979, *Icarus*, **38**, 166.
Fegley, B., Jr., and Prinn, R. G. 1985, *Ap. J.*, **299**, 1067.
———. 1986, *Ap. J.*, **307**, 852.
———. 1987, paper presented at the meeting on The Origin and Evolution of Planetary and Satellite Atmospheres. (Tucson, 1987 March 10–14).
———. 1988, *Ap. J.*, in press.
Fegley, B., Jr., Prinn, R. G., Hartman, H., and Watkins, G. H. 1986, *Nature*, **319**, 305.
Fink, U., and Larson, H. P. 1978, *Science*, **201**, 343.
———. 1979, *Ap. J.*, **233**, 1021.
Flasar, M., and Gierasch, P. 1977, in *Proc. Symposium on Planetary Atmospheres*, ed. A. Vallance-Jones (Ottawa: Royal Society of Canada), p. 85.
Fox. K., Owen, T., Mantz, A. W., and Rao, K. 1972, *Ap. J. (Letters)*, **176**, L81.
Friedman, I., and O'Neill, J. R. 1977, in *Data of Geochemistry*, 6th ed., USGS Prof. Paper 440-KK.
Gat, J. R. 1980, in *Handbook of Environmental Isotope Geochemistry*, Vol. **1**, ed. P. Fritz and J. Ch. Fontes (Amsterdam: Elsevier), p. 21.
Gautier, D., Bezard, B., Marten, A., Baluteau, J. P., Scott, N., Chedin, A., Kunde, V., and Hanel, R. 1982, *Ap. J.*, **257**, 901.
Gautier, D., Conrath, B., Hanel, R., Kunde, V., Chedin, A., and Scott, N. 1981, *J. Geophys. Res.*, **86**, 8713.
Gautier, D., and Owen, T. 1983, *Nature*, **304**, 691.
Geiss, J., and Bochsler, P. 1981, in *Solar Wind Four*, (Lindau: MPAE), p. 403.
Geiss, J., and Reeves, H. 1972, *Astr. Ap.*, **18**, 126.
Glassgold, A. E., Huggins, P. J., and Langer, W. D. 1985, *Ap. J.*, **290**, 615.
Glushko, V. P., *et al.*, eds. 1965–1981, *Thermodynamic Constants of Matter*, Vols. **1–10** (Moscow: High-Temperature Institute).
Glushko, V. P., Gurich, L. V., Bergman, G. A., Veitz, I. V., Medvedev, A. A., Khachkuruzov, G. A., and Yungman, V. S., eds. 1978–1982, *Thermodynamic Properties of Individual Substances*, Vols. **1–4**, (Moscow: High-Temperature Institute).
Gutman, J. R. 1953, *J. Phys. Chem.*, **57**, 309.
Harrison, L. G., and McDowell, C. A. 1953, *Proc. Roy. Soc. London A*, **220**, 77.
Hsu, D. S. Y., and Manuccia, T. J. 1980, *Appl. Phys. Letters*, **36**, 714.
Hubbard, W. B., and MacFarlane, J. J. 1980, *Icarus*, **44**, 676.
Hubbard, W. B., and Stevenson, D. J. 1984, in *Saturn*, ed. T. Gehrels and M. S. Matthews (Tucson: University of Arizona Press), p. 47.
Jansco, G., and Van Hook, W. A. 1974, *Chem. Rev.*, **74**, 689.
Kaye, J. A. 1987, *Rev. Geophys.*, in press.
Kaye, J. A., and Strobel, D. F. 1983, *Icarus*, **54**, 417.
Keenan, J. H., Keyes, F. G., Hill, P. G., and Moore, J. G. 1969, *Steam Tables* (New York: Wiley).
Kelley, K. K. 1937, *Contributions to the Data on Theoretical Metallurgy*, Vol. **7**, *The Thermodynamic Properties of Sulphur and Its Inorganic Compounds* (Washington DC: US Bureau Mines Bull., No. 406).
———. *Contributions to the Data On Theoretical Metallurgy*, Vol. **13**, *High-Temperature Heat-Content, Heat-Capacity, and Entropy Data for the Elements and Inorganic Compounds* (Washington, DC: US Bureau Mines Bull. No. 584).
Kelley, K. K., and King, E. G. 1961, *Contributions to the Data on Theoretical Metallurgy*, Vol. **14**, *Entropies of the Elements and Inorganic Compounds* (Washington DC: U.S. Bureau Mines Bull., No. 592).
Kemball, C. 1952, *Proc. Roy. Soc. London A*, **214**, 413.
Kerr, J. A., and Parsonage, M. J. 1976, *Evaluated Kinetic Data on Gas Phase Hydrogen Transfer Reactions of Methyl Radicals* (London: Butterworths).
Kirshenbaum, I. 1951, *Physical Properties and Analysis of Heavy Water* (New York: McGraw-Hill).
Kirshenbaum, I., and Urey, H. C. 1942, *J. Chem. Phys.*, **10**, 706.
Klein, F. S. 1975, *Ann. Rev. Phys. Chem.*, **26**, 191.
Knacke, R. F., Kim, S. J., Ridgway, S. T., and Tokunaga, A. T. 1982, *Ap. J.*, **262**, 388.
Kunde, V., Hanel, R., Maguire, W., Gautier, D., Baluteau, J. P., Marten, A., Chedin, A., Husson, N., and Scott, N. 1982, *Ap. J.*, **263**, 443.
Lacy, J. H., Larrabee, A. I., Wollmann, E. R., Geballe, T. R., Townes, C. H., Bregman, J. D., and Rank, D. M. 1975, *Ap. J. (Letters)*, **198**, L145.
Larson, H. P., Davis, D. S., Hofmann, R., and Bjoraker, G. L. 1984, *Icarus*, **60**, 621.
Larson, H. P., Fink, U., and Treffers, R. R. 1978, *Ap. J.*, **219**, 1084.
Laufer, A. H., and McNesby, J. R. 1965, *Canadian J. Chem.*, **43**, 3487.
Lee, J. H., Michael, J. V., Payne, W. A., Whytock, D. A., and Stief, L. J. 1976, *J. Chem. Phys.*, **65**, 3280.
Lellouch, E., and Destombes, J. L. 1985, *Astr. Ap.*, **152**, 405.
Lewis, J. S., and Fegley, B., Jr. 1984 *Space Sci. Rev.*, **39**, 163.
Lewis, J. S., and Prinn, R. G. 1984, *Planets and Their Atmospheres* (New York: Academic Press).
Lindal, G. F., *et al.* 1981, *J. Geophys. Res.*, **86**, 8721.
Macy, W., Jr., and Smith, W. H. 1978, *Ap. J. (Letters)*, **222**, L73.
Marshall, P., and Fontijn, A. 1986, *J. Chem. Phys.*, **85**, 2637.
Mason, B. J. 1971, *The Physics of Clouds*, (2d ed.; Oxford: Clarendon Press).
Massie, S. T., and Hunten, D. M. 1982, *Icarus*, **49**, 213.
Mauersberger, K. 1987, *Geophys. Res. Letters* **14**, 80.
McKellar, A. R. W., Goetz, W., and Ramsay, D. A. 1976, *Ap. J.*, **207**, 663.
Melander, L. 1960, *Isotope Effects on Reaction Rates* (New York: Ronald Press).
Michael, J. F., Sutherland, J. W., and Klemm, R. B. 1986, *J. Phys. Chem.*, **90**, 497.
Noll, K. S., Knacke, R. F., Geballe, T. R., and Tokunaga, A. T. 1988, *Ap. J.*, in press.
Pamidimukkala, K. M., Rogers, D., and Skinner, G. B. 1982, *J. Phys. Chem. Ref. Data*, **11**, 83.
Persky, A. 1973, *J. Chem. Phys.*, **59**, 3612.
Persky, A., and Klein, F. S. 1966, *J. Chem. Phys.*, **44**, 3617.
Prinn, R. G., and Barshay, S. S. 1977, *Science*, **198**, 1031.
Prinn, R. G., and Fegley, B., Jr. 1981, *Ap. J.*, **249**, 308.
Prinn, R. G., Larson, H. P., Caldwell, J. J., and Gautier, D. 1984, in *Saturn*, ed. T. Gehrels and M. S. Matthews (Tucson: University of Arizona Press), p. 88.
Prinn, R. G., and Olaguer, E. P. 1981, *J. Geophys. Res.*, **86**, 9895.
Prinn, R. G., and Owen, T. 1976, *Jupiter*, ed. T. Gehrels (Tucson: University of Arizona Press), p. 319.

Richet, P., Bottinga, Y., and Javoy, M. 1977, *Ann. Rev. Earth Planet. Sci.*, **5**, 65.
Rinsland, C. P., Devi, V. M., Flaud, J. M., Camy-Peyret, C., Smith, M. A. H., and Stokes, G. M. 1985, *J. Geophys. Res.*, **90**, 10719.
Romani, P. N. 1986, Ph.D. thesis, University of Michigan.
Shabur, V. N., Katashinskii, A. S., Titova, I. S., and Koval'chuk, D. S. 1969, *High Temp.*, **7**, 338.
Singleton, J. H., Roberts, E. R., and Winter, E. R. S. 1951, *Trans. Faraday Soc.*, **47**, 1318.
Smith, I. W. M., and Zellner, R. 1974, *J. Chem. Soc. Faraday Trans. II.*, **70**, 1045.
Stone, P. H. 1976, in *Jupiter*, ed. T. Gehrels (Tucson: University of Arizona Press), p. 586.
Strobel, D. F. 1985, in *The Photochemistry of Atmospheres*, ed. J. S. Levine (New York: Academic Press), p. 393.
Stull, D. R., Westrum, E. F., Jr., and Sinke, C. G. 1969, *The Chemical Thermodynamics of Organic Compounds* (New York: Wiley).
Thyagarajan, G., Sundaram, S., and Cleveland, F. F. 1960, *J. Molec. Spectrosc.*, **5**, 307.
Tokunaga, A. T., Beck, S. C., Geballe, T. R., Lacy, J. H., and Serabyn, E. 1981 *Icarus*, **48**, 283.
Tokunaga, A. T., Knacke, R. F., Ridgway, S. T., and Wallace, L. 1979, *Ap. J.*, **232**, 603.
Tomasko, M. G., West, R. A., Orton, G. S., and Teifel, V. G. 1984, in *Saturn*, ed. T. Gehrels and M. S. Matthews (Tucson: University of Arizona Press), p. 150.
Trafton, L., and Ramsay, D. A. 1980, *Icarus*, **41**, 423.
Trauger, J. T., Roesler, F. L., Carlton, N. P., and Traub, W. A. 1973, *Ap. J. (Letters)*, **184**, L137.
Trauger, J. T., Roesler, F. L., and Mickelson, M. E. 1977, *Bull. AAS*, **9**, 516.
Tsang, W., and Hampson, R. F. 1986, *J. Phys. Chem. Ref. Data*, **15**, 1087.
Urey, H. C. 1947, *J. Chem. Soc.*, (London), p. 562.
Wagman, D. D., Evans, W. H., Parker, V. B., Halow, I., Bailey, S. M., and Schumm, R. H. 1968, *Selected Values of Chemical Thermodynamic Properties: Tables for the First Thirty-Four Elements in the Standard Order of Arrangement* (NBS Tech. Note No. 270-3).
Warnatz, J. 1984, in *Combustion Chemistry*, ed. W. C. Gardiner, Jr. (New York: Springer Verlag), p. 197.
Weber, J., and Laidler, K. J. 1951, *J. Chem. Phys.*, **19**, 1089.
West, R. A., Strobel, D. F., and Tomasko, M. G. 1986, *Icarus*, **65**, 161.
Weston, R. E., Jr., and Bigeleisen, J. 1952, *J. Chem. Phys.*, **20**, 1400.
Yaakov, Y. B., Persky, A., and Klein, F. S. 1973, *J. Chem. Phys.*, **59**, 2415.

B. FEGLEY, JR.: Building 54-1822, Department of Earth, Atmospheric, and Planetary Sciences, Massachusetts Institute of Technology, Cambridge, MA 02139

R. G. PRINN: Building 54-1824, Department of Earth, Atmospheric, and Planetary Sciences, Massachusetts Institute of Technology, Cambridge MA 02139